LA--12223-PR

DE92 008207

Health, Safety, and Environment Division

Annual Report
1990

Complied by
Carol Wade

DISCLAIMER

Contents

Abstract

The primary responsibility of the Health, Safety, and Environment (HSE) Division at the Los Alamos National Laboratory is to provide comprehensive occupational health and safety programs, waste processing, and environmental protection. These activities are designed to protect the worker, the public, and the environment. Meeting these responsibilities requires expertise in many disciplines, including radiation protection, industrial hygiene, safety, occupational medicine, environmental science and engineering, analytical chemistry, epidemiology, and waste management. New and challenging health, safety, and environmental problems occasionally arise from the diverse research and development work of the Laboratory, and research programs in HSE Division often stem from these applied needs. These programs continue but are also extended, as needed, to study specific problems for the Department of Energy. The results of these programs help develop better practices in occupational health and safety, radiation protection, and environmental science.

Industrial Hygiene

Visualizing Air Circulation Patterns in Plutonium Laboratories Using Neutrally Buoyant Bubbles

Author: C. I. Fairchild, HSE-5
Technical Assistance: R. C. Lopez, HSE-5
Group: Industrial Hygiene, HSE-5
Funding Organization: Department of Energy, Bush Amendment Technical Safety Appraisal (TAS) Funds

Introduction

This work tested the feasibility of a new method for measuring air circulation in laboratories. The purpose was to improve sampler placement and to document the rationale for that placement.

A previous study of ventilation rates conducted in three plutonium laboratories[1] showed that air samplers can be located effectively in accordance with known air circulation. During the study, air circulation was determined qualitatively by tracking and videotaping the travel of neutral buoyancy bubbles. As a continuation of that study, we investigated the feasibility of a similar method to quantitatively determine and record air circulation patterns.

Concept

Airflow patterns in a room can be visualized by following the movement of neutrally buoyant bubbles. Previously, researchers used smoke or a large number of small bubbles to track air currents. Smoke has undesirable thermal properties and its particles are too rapidly diffused in small-scale turbulence. Scientists who released numerous smaller neutrally buoyant bubbles of 1-2-mm dia found them confusing and difficult to follow. By releasing one or a few large bubbles we eliminate the drawbacks of these earlier techniques.

The requirements for a system that produces and follows single, large bubbles are

- bubble material that forms long-lasting bubbles;
- a generator capable of controlling the size, fill gas composition, and release rate of the bubbles; and
- a tracking system capable of determining the position of a bubble in three dimensions, and providing a permanent record of the tracks of a sufficient number of bubbles to determine major airflow paths.

Uniform size is required for neutral buoyancy because the pressure of the fill gas must exactly balance the mass of bubble film and displaced air. Factors that remain constant such as densities of air, fill gas, and film material may be neglected when comparing different size bubbles. The buoyancy of the gas is proportional to the volume of the sphere, whereas the mass of the film is proportional to the bubble surface area and thickness. Therefore, the net buoyancy for similar bubbles changes as the ratio of the sphere volume to the sphere surface area multiplied by the thickness:

Ratio = 4/3*Pi*r3 / 4*Pi*r2*t = r/3t.

Thus, the buoyancy changes as r/3t and, assuming a constant fill gas composition, a series of bubbles must be approximately the same size to meet the neutral buoyancy requirement.

In this method, a quantitative record of bubble tracks is made and a qualitative record of air circulation can also be obtained by videotaping the bubbles. Either a triangulation or ranging technique may be used. The latter is more cost effective and simpler in use, but requires more sophisticated equipment. For the ranging technique, a single sighting station suffices to provide data for bubble position calculation if an aimed laser or other device can provide distance measurement. The triangulation technique utilizes two sighting stations and no distance or ranging information. Two pointing devices provide angular data to calculate the bubble position.

Experimental

A bubble generator has been developed that produces uniformly sized bubbles up to 4-in. dia, filled with a helium/air mixture. An operator can adjust the He/air mixture, change the mixture flow rate, and control the rate of release of bubbles, all from a control panel within 20 ft. The bubble source material is a commercial polymer liquid.

A triangulation data acquisition and analysis system was built to conduct proof of concept experiments for tracking and data reduction. With this system, bubbles released from the generator may be tracked as they drift with air currents by two camcorders mounted on instrumented tripods. Each camcorder tripod has two single-turn potentiometers, mounted orthogonally to one another, that attenuate an applied dc voltage according to the direction the camcorders are pointed. The attenuated signal is transmitted to a computer where an x-y-z plot of the bubble's track is shown in real time. This plot updates the bubble position every 5 sec.

The tracks of all bubbles are shown so that similar paths are emphasized.

Operators aim camcorders by imaging the bubble in a target circle drawn on the center of a TV monitor screen to provide easier tracking than sighting through the camcorder. Operators depress foot switches when they have centered the bubble on the monitor. Only when foot switches are depressed by both operators are data transmitted to the computer, thus eliminating off-target data. One of the operators operates the bubble generator.

In addition to the real-time plot of bubble tracks, data are later available from disk. These data can be used in an existing program to produce a finished, annotated graph of the bubble tracks. Thus, two permanent records of the tracking are available: the videotape of the experiments and the stored data or resultant graphs.

Tracking experiments were conducted with the triangulation system in three separate laboratories: a school gymnasium, a small laboratory, and a large plutonium laboratory. Development work was conducted in the first two rooms and the last was an operating plutonium laboratory in which ventilation studies had previously been conducted.[1,2] Consequently, in the plutonium laboratory the air circulation patterns were known and were useful for checking the similarity of the bubble tracks to the previously measured patterns.

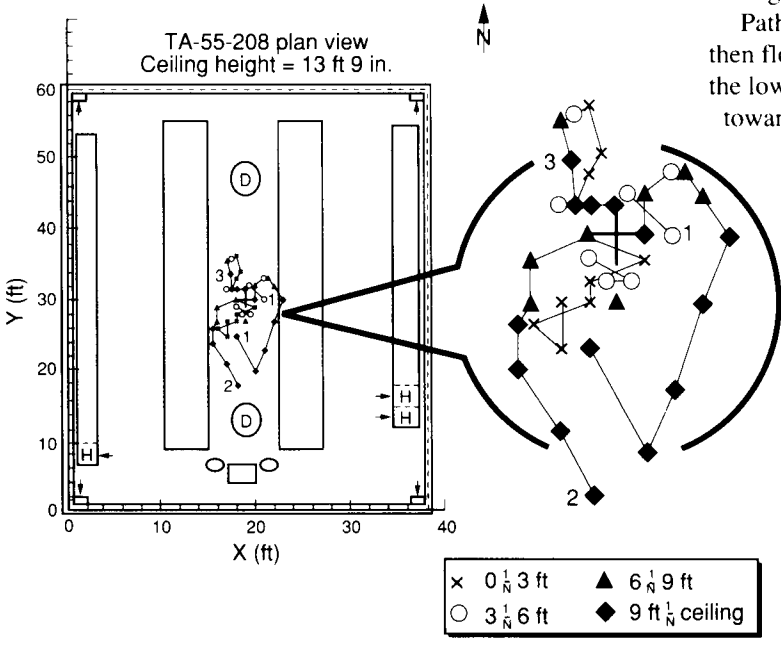

Fig. 1. Bubble tracks traced in a plutonium laboratory.

Discussion

Figure 1 is an illustration of bubble tracks obtained in the plutonium laboratory. The plan view of the room shows the four major glove boxes and a transverse tunnel that was located above the glove boxes. The two circles with the enclosed Ds represent the two ceiling diffuser air inlets, and the four rectangles in the corners represent the floor-mounted room air exhausts. The bubble tracking equipment, represented at the south end of the room, consists of two tripods (ovals) and a rolling table (rectangle). In this case the bubble generator was located 3.5 ft above the floor at the cross near the center of the room to simulate a center release as used in the ventilation experiments in this lab. The elevation of each point of the bubble tracks is indicated by the symbol used for the point. The elevation symbols are indexed in the figure. Each of the dotted lines, tracks 1, 2, and 3, represents the general paths of a number of bubbles.

Track 1 represents the path of the majority of bubbles. This path starts from the release point (coordinates x = 19, y = 28), travels to the northeast to a point under the transverse tunnel, then reverses course toward the southeast and upward over the right glove box. Bubbles continued to rise and travel fairly rapidly toward the south diffuser, but when a few feet from the diffuser, were caught by supply air blown horizontally along the ceiling toward the northwest. Most bubbles that were entrained in the high-velocity outflow impacted the ceiling or broke because of the acceleration.

Path 2 was similar, except that the bubbles dropped lower, then floated southwest. They often made a circle or spiral in the low velocity air down low, then moved upward and toward the south diffuser.

Path 3 shows the track of one unique bubble. Initially, the bubble meandered in the stagnant air near the floor, but then it rose almost vertically and passed to the north over the transverse tunnel. Upon reaching the north side of the transverse tunnel, this bubble dropped vertically, evidently in a downflow from the north diffuser. Surprisingly, it then drifted south near the floor under the tunnel resulting in a complete loop around the transverse tunnel that it repeated three times before breaking.

Tests in the plutonium lab revealed airflow patterns similar to those determined in previous aerosol experiments and numerical modeling for the room. Specifically, the upward travel of air shown in Paths 1 and 2 was a duplicate of patterns seen previously in which much of the air from the central portion of the room was induced upward into the outflow from the diffusers. The loop circulation of Path 3 was also predicted in the computational fluid dynamics code, SOLA-DM, simulation for aerosol release at that location.

Although developing a ranging system was not within the scope of the concept proving project, we briefly investigated the feasibility of such a system employing a single station and single operator. Laser return from fluorescence-enhanced

bubbles might be used to determine the distance from camcorder to bubbles. Laser experts indicate that a low-power argon laser could be used to range on fluorescent bubbles and transmit distance information to the computer. We determined by experimentation that up to 0.05% by volume of sodium fluorescein could be dissolved in bubble material without compromising durability of the bubbles. Laser experts estimated this percentage sufficient to produce adequate laser reflection.

In addition to providing spectral reflection for ranging, fluorescence-enhanced bubbles would be enhanced visibly to provide better targets for the operator. Moreover, because the laser beam divergence angle would be small, the bubble would glow when the laser was on target When thus signaled, the operator would engage the foot switch. Aided by these features, operators would be less likely to enter erroneous data.

Conclusions

A system for mapping the air circulation in laboratories has been developed. The apparatus tested during this study was intended primarily to prove the concept and did not represent the optimum equipment or method for measuring the airflow. Nonetheless, the method was found to be practical for documenting air circulation patterns.

References

1. C. I. Fairchild, M. I. Tillery, F. R. Krause, W. S. Gregory, J. B. Bennett, and R. C. Lopez, *Health-Related Effects of Different Ventilation Rates in Plutonium Laboratories, Final Report*, Los Alamos National Laboratory report, LA-11948-MS (Jan 1991).
2. C. I. Fairchild, M. I. Tillery, F. R. Krause, and W. S. Gregory, "A Study of Ventilation Air Exchange Rates in Hazardous Materials Laboratories," in *Ventilation* **88**, James H. Vincent, Ed. (Pergamon Press, Oxford, 1989) pp. 269-277.

Computational Fluid Dynamics and Aerosol Modeling of a Plutonium Laboratory at the Rocky Flats Plant

Authors: C. I. Fairchild (HSE-5) and W. S. Gregory (N-6)
Technical Assistance: R. C. Lopez (HSE-5)
Groups: Industrial Hygiene, HSE-5; Safety Assessment, N-6
Funding Organization: Department of Energy, Bush Amendment Technical Safety Appraisal Funds

Introduction

Several groups in HSE Division have been studying airflow circulation patterns in plutonium handling laboratories for a number of years. The need for these studies centers on proper placement of alarms and detectors within a room where hazardous materials are processed. Generally, these rooms are large and have many obstructions to airflow. In addition to the interior obstacles, multiple air supply and exhaust systems are located throughout the Laboratory. Size and configurations of these rooms result in complex air circulation patterns.

The Industrial Hygiene Group (HSE-5) has used experimental means to determine airflow patterns in several of these rooms at Los Alamos and at the Rocky Flats Plant (RFP).[1,2,3] These studies basically consist of measuring the inflow and outflow air quantities, visualizing airflow, and injecting and subsequently detecting aerosol at specific locations. Aerosol particle detectors, thermal anemometers, sensitive wind vanes, and neutrally buoyant bubble tracking have provided aerosol distribution data, velocity magnitude and direction, and overall air circulation patterns in each room. Using these tools, we can obtain information such as aerosol mass concentrations and velocity field values throughout the room. However, the experiments are time consuming and expensive. For this reason, N-6 and HSE-5 personnel have supplemented the experimental measurements with computational fluid dynamics (CFD) techniques. Based on the results of the previous experiments and applications of CFD modeling to Los Alamos and Rocky Flats laboratories, CFD techniques have been applied to a large laboratory at RFP—Room 3305 of Building 371.

The objective was to determine whether CFD techniques could model a large, complex laboratory to produce results that compared well with experimental results from the same room. The report[4] of the comparison contains considerable material describing the code and analysis of the input requirements, as well as extensive color output from the CFD simulation. Consequently, the contents of that report will be condensed here and only the conclusions will be presented in full.

Room Description

A plan view of Room 3305 (Fig. 1) shows the glove box layout as well as other obstacles, and also shows the 10 ceiling-mounted air supply plenums and 14 floor-mounted exhaust plenums. The airflows from all supply plenums and into all exhaust plenums were measured with thermal anemometer velocity traverses. The volume airflows ranged from 479 ft^3/min to 949 ft^3/min for the supply airflows from individual plenums, with the average coefficient of variation (COV) of the measurements for each air-supply plenum being ~14%. The range of volume airflow from the 14 exhausts ranged from 326 ft^3/min to 716 ft^3/min, with the COV of measurements of individual exhaust plenums up to 34%. The large COV for the exhaust measurements was due primarily to the turbulence of the room air as it entered the exhaust fixtures. These airflow measurements served as input into the CFD code.

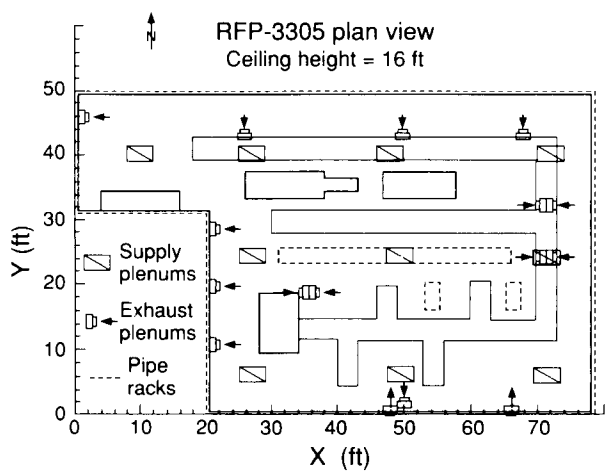

Fig. 1. Plan view of Room 330 showing glove box layout, 10 ceiling-mounted air supply plenums, and 14 floor-mounted exhaust plenums.

Code Description

The CFD code used in the study, SOLA-DM, is highly vectorized for efficient performance on Cray computers. It is a three-dimensional, finite difference, time-explicit code that evolved from the marker and cell method. This Eularian code is designed to solve the time-dependent Navier-Stokes hydrodynamic equations. The code was applied to a model consisting of ~35,000 cells, 10 air inflows, 14 air outflows, 5 variable-size glove boxes, and miscellaneous obstructions. The plan view of the model is shown in Fig. 2, with the cell grid overlying the obstacles' outlines.

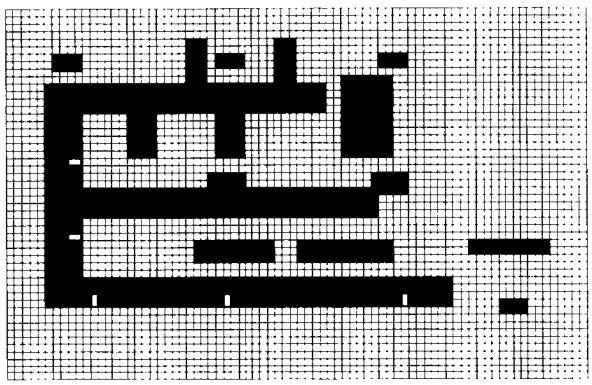

Fig. 2. Plan view of the ~35,000-cell model of the RFP laboratory with overlaid grid.

CFD modeling of the room proved feasible; typical calculations to achieve steady-state airflow patterns required ~15-20 minutes of Cray central processing time. A reasonable amount of computation time (950 CPUs or 7.5 s/cell per cycle) was required to achieve steady-state airflow patterns. Three ventilation rates (4.7, 9.3, and 16.5 air changes per hour) were analyzed along with the injection of tracer particles at three locations within the room. Results of these calculations were in the form of color velocity vector cross sections, perspective particle location plots, and particle motion movies.

Results

Three-dimensional code output simulations of tracer particle distribution were compared to contour plots of aerosol concentration from experiments conducted in the same room. Although the simulations did not exhibit dispersion of particles over the entire room as did experimental results, most of the simulations were in qualitative agreement with the experimental aerosol distribution. We devised a quantitative rating scheme, based on the qualitative comparison of aerosol concentration and particle movement, that indicated that the code provided a good simulation of the experimental results in 63% of the cases evaluated. Variance of the room exhaust measurements may have contributed significantly to the disagreement in the comparison.

A separate comparison was made of particle number concentration as a function of elapsed release time at one position in the laboratory for four different release conditions. The number concentration measured by a laser particle counter (LPC) during the experiments was compared with the number concentration of particles computed by the code for the identical volume. The number of particles injected in the code calculations was made three orders of magnitude lower than the actual aerosol number concentration to reduce computation time. Even so, the shape of the number concentration curves as a function of time were similar for the code output and experiments until the final stage of the simulation. In this stage, which is the concentration decay phase after the cessation of particle injection and cessation of aerosol generation, two of the four simulations differed from experimental results by factors of >2. The other two simulations agreed with experiments within 10%.

Conclusions

A qualitative comparison of the SOLA-DM simulation against experiments in the RFP laboratory indicates that the code compares well for ~63% of the features evaluated. The simulation for RFP Room 3305 is not as good as the previous comparison in two Los Alamos laboratories[1,2] in which the qualitative comparison indicated ~75% agreement between the analytical simulation and the experiments. The difference between the results for RFP and the earlier cases may be explained by both the greater variance of exhaust outflow measurements at RFP and the greater size and complexity of the RFP laboratory.

A comparison of particle number concentration at a single location in the room indicates that the progress of an aerosol release was well simulated by the code except for the decay phase of the release. In two of four comparisons, the SOLA-DM simulation of local concentration decay rates agreed well with the experiments, but in two cases the simulated decay rates differed by factors of >2 from the experimental results for unknown reasons.

When tracer particles were injected into SOLA-DM calculations to simulate the corresponding experimental releases, a large fraction of the simulated particle cloud was concentrated in less than one-third of the room. In contrast, the actual aerosol distribution was more diffuse and it was spread throughout the room, although regions of high concentration were present. The difference may be attributable to the lack of a turbulence model in the code.

References

1. C. I. Fairchild, M. I. Tillery, F. R. Krause, W. S. Gregory, J. B. Bennett, and R. C. Lopez, "The Health-Related Effects of Different Ventilation Rates in Plutonium Laboratories," Los Alamos National Laboratory report LA-11948-MS (Jan 1991).
2. C. I. Fairchild, M. I. Tillery, F. R. Krause, and W. S. Gregory, "A Study of Ventilation Air Exchange Rates in Hazardous Materials Laboratories," in *Ventilation* **88**, James H. Vincent, Ed. (Pergamon Press, Oxford, 1989), pp. 269-277.
3. C. W. Hirt, L. R. Stein, and R. C. Scripsick, "Prediction of Air Flow Patterns in Ventilated Rooms," Los Alamos National Laboratory, report LA-UR-79-1550 (1979).
4. W. S. Gregory and C. Fairchild, "Computational Fluid Dynamics and Aerosol Modeling of Room 3305, Building 371, of the Rocky Flats Plant," November, 1990, Los Alamos National Laboratory document.

Filter Test Equipment Modernization

Authors: J. A. McIntyre and R. C. Scripsick
Technical Assistance: A. G. Trujillo, R. C. Lopez, and T. A. Trujillo
Group: Industrial Hygiene, HSE-5
Funding Organization: US Army, Product Assurance Directorate

Introduction

This program will provide the Army's Product Assurance Directorate (PAD), Edgewood, Maryland, with two modern filter penetration measuring systems for testing high-efficiency particulate air (HEPA) filters. Filters with rated flows from 5 to 2000 cubic feet per minute (ft^3/min) will be tested. A High-Flow Alternative Test System (HFATS) will be supplied to test filters with rated flows from 500 ft^3/min to 2000 ft^3/min. This system was designed and evaluated in a 5-year program at Los Alamos for the US Department of Energy (DOE). In addition, a Low-Flow Alternative Test System (LFATS) will be supplied to test filters with rated flows from 5 ft^3/min to 250 ft^3/min. The LFATS development will be based on data collected to develop the HFATS. Both the HFATS and the LFATS use di-(2-ethylhexyl) phthalate (DEHP) as the challenge aerosol material and could potentially be converted for use with other test aerosol materials.

High-Flow Alternative Test System

We monitored fabrication of the HFATS test stand by the Chamberlin Manufacturing (MRC) plant in Baltimore, Maryland, through CY 1990. MRC's initial project schedule identified a completion date for each phase of the contract. Final acceptance of the HFATS at the PAD facility was initially scheduled for the end of January in 1990. The project milestones included the following:

- MRC's final design—subject to approval by HSE-5's Research and Development Section;
- the Research and Development Section's approval of the final design;
- completion of the HFATS test stand;
- assembly and test of the HFATS test system at MRC;
- installation and acceptance testing of the HFATS at PAD; and
- MRC's documentation, operating manuals, and engineering prints of the HFATS test stand by MRC.

The HFATS test stand was completed in June 1990, initial proof testing performed at the MRC facility in July and September, and installation, acceptance, and proof testing completed at the PAD facility during October 1990. A few minor details requiring MRC's attention, including lowering the background concentration, installing a computer stand, and mounting the frequency adjustment for the main blower, delayed the final acceptance of the HFATS test stand to the first quarter of CY 1991.

Low-Flow Alternative Filter Test System

In CY 1990, funding to Los Alamos continued for the development, procurement, fabrication, laboratory proof testing of the LFATS test equipment and for completion of the LFATS documentation and operations manuals. Jeff Taylor of PAD visited Los Alamos to further discuss the contract for the LFATS and the commitment of 1990 funding.

The development of the LFATS is based on the data collected during the DOE program to develop the HFATS and requires the design of a LFATS aerosol generator based on that of the HFATS generator. LFATS generator testing was performed primarily at PAD during the last quarter of CY 1990 by installing the HFATS test equipment on the Q233 test system. Preliminary testing indicated that the generator, diluter/sampler, and laser spectrometer system provided the desired aerosol concentration and particle size distribution. The aerosol charge distribution measurements will be performed at Los Alamos to determine the aerosol neutralization capacity required to standardize the charge on the aerosol challenge. LFATS test equipment operation will be adjusted and some software modification will be necessary, according to LFATS test results.

The design, procurement, and fabrication of the LFATS test equipment, including the generator, aerosol neutralizers, diluter/sampler and laser spectrometer system, has been completed.

Technical Support for Filter Test Facilities

Authors: J. A. McIntyre and R. C. Scripsick
Technical Assistance: A. G. Trujillo and R. C. Lopez
Group: Industrial Hygiene, HSE-5
Funding Organization: Department of Energy, Albuquerque Operations Office, Waste Management and Transportation Division, Interim Waste Operations

Introduction

This program provides technical support to the DOE Filter Test Facilities (FTFs) by carrying out both scheduled activities and helping solve special problems that arise. For several years, we have been initiating and reviewing round-robin tests (RRT), summarizing yearly activities of the FTFs, and providing technical consulting services to the FTFs. In addition, Los Alamos is available to provide technical assistance to the DOE and FTFs in addressing special problems. For 1990, we helped transfer the High-Flow Alternative Test System (HFATS) to the FTFs. In-place testing is scheduled for FY 1991.

Round-Robin Test Program

The RRT program monitors the consistency of FTF measurements by circulating six high-efficiency particulate air (HEPA) filters through each of the three FTFs. One FTF serves as a reference site, testing the filters before and after they are sent to other FTFs. This reference testing documents that the test filters have not been affected by the test program; it also reports on the internal consistency of the reference FTF. The goals of the RRT program include (1) documenting measurement consistency among and within individual FTFs; (2) suggesting areas where improvement of FTF measurement accuracy and precision may be possible; and (3) monitoring and documenting the effects of FTF measurements on implementation of these proposed improvements.

In 1990, Los Alamos coordinated two RRTs, began to interpret their results, and identified trends in the data collected over the history of the RRT program. We selected, for the 1990 RRT test, filters with higher average penetration; filters with 0.03% penetration were rejected. Study of the test filters with higher average penetrations will provide data to evaluate measurement consistency of the FTFs at the rejection level. Analysis of the FY 1990 RRT data is in progress.

FTF Semiannual Report Summary

In the fall and spring, each FTF issues a report detailing numbers of filters accepted and rejected for each shipment during the previous six months. Los Alamos examines these data to assess individual manufacturer's FTF test consistency and filter quality. With this evaluation, we hope to provide a standard against which to judge FTF performance and provide information on performance of filters being used in DOE facility ventilation exhausts and other airflow systems.

To meet the first objective, we assess the consistency of measurements among FTFs. By combining these results with those of the *ongoing* DOE RRT program, we document the consistency of measurements among all FTFs for DOE.

To meet the second objective, we measure the quality of filters presented to the DOE FTFs and installed in DOE facilities. The quality of filters received by the FTFs affects their operating costs and contributes to potential delays in the mission of the DOE contractor purchasing and installing the filters. Analysis of FTF data from FY 1990 is in progress.

Special Technical Assistance

Los Alamos staff provides assistance on technical problems that affect individual FTFs and the FTFs collectively. These problems deal with compliance to FTF standards, potential improvements that are indicated by the RRT program or the review of FTF data, or special problems that the FTFs encounter during operation. Los Alamos involvement in solving technical problems has included designing and modifying equipment, proof-testing modifications, analyzing data collected by the FTF, surveying and interpreting literature, and developing technical positions on FTF issues.

HFATS Support Activities

Los Alamos has developed an alternative to the current filter test system (Q107) used to test size 4 (500 ft^3/min rated flow) and larger nuclear-grade HEPA filters at DOE FTFs. This new test system, called the HFATS, consists of an air-operated nozzle aerosol generator and a laser aerosol spectrometer (LAS)/diluter monitoring system. Four major activities aided the further transfer of the HFATS: (1) Oak Ridge fabricated the improved diluter/samplers and delivered them to the FTFs, (2) the three FTFs installed and extensively proof-tested the HFATS, (3) FTF personnel were trained to operate and test the HFATS, and (4) all three FTFs initiated and completed an HFATS RRT.

The objective of the HFATS RRT was to collect test data using the Q107 penetrometer and HFATS at each FTF for evaluation of the proposed HFATS test method. The initial HFATS RRT design was modeled after the ongoing RRT test program. Los Alamos obtained a set of 12 size-5 (1000 ft^3/min rated flow) filters from the Rocky Flats FTF. The 12 filters were randomly selected from a set of 100 size-5 filters that were previously tested and demonstrated to have higher than average penetration measurements. The filters were tested by both the Q107 penetrometer and HFATS test methods at all three FTFs. Analysis of the data from the HFATS RRT is in progress.

Performance of Fibrous Filter at Low Flows

Authors: R. C. Scripsick and W. C. Hinds
Technical Assistance: T. M. Trujillo and A. G. Trujillo
Group: Industrial Hygiene, HSE-5
Funding Organizations: The Nuclear Materials Office and Los Alamos National Laboratory, Health, Safety, and Environment Division, Special Nuclear Materials Laboratory Project

Introduction

In facilities that handle highly hazardous materials, high efficiency fibrous filters are often the last line of protection between highly contaminated areas and the environment. These filters must provide protection during off-normal conditions as well as during normal operation. Filter performance during normal operation is well understood. However, almost no experimental data exist on the performance of these filters at flows well below rated flow. The objective of this program is to investigate the performance of fibrous filters under the nonstandard condition of low flow. Low flow is defined here as flow at or below 20% of the full-rated filter flow.

Filters are exposed to low flows in many situations, some of which include ventilation system balancing and start-up, filter change-out, in-place filter testing, and loss of electrical power. During loss of electrical power, many Department of Energy (DOE) nuclear facilities undergo passive safe shutdown (Post, 1991), in which ventilation flow is governed by free convection. Under passive safe shutdown, filter flow is highly variable, can reverse direction, and may fall to zero.

The rate of material release from a facility is related to filter penetration as follows:

$$R = P\,C\,Q, \qquad (1)$$

where

- R = flux of material penetrating filter, number of particles per unit time;
- P = filter penetration;
- C = challenge concentration, particles/unit volume; and
- Q = flow rate, unit volume/unit time.

This relationship shows that as penetration decreases, so does the release rate and that release rate is a maximum when P equals its maximum of 1. Fibrous filtration theory predicts that penetration decreases with flow in the region where diffusion-collection dominates. Consequently, as flow is reduced during passive safe shutdown, release rate is expected to decrease.

A recent review (Scripsick and Hinds, 1990) of the performance of the nuclear-grade, high-efficiency particulate air (HEPA) filters used in DOE nuclear facilities showed deviations from filtration theory. These deviations raise questions about the true functional dependence of penetration on flow and may predict the increase of penetration as flow drops. If penetration is found to increase with decreasing flow, then the precise functional dependence of penetration on flow becomes critical. Initial suspicions are that the deviations are a result of weak areas in the filter that cause the filter to perform at low flows as a filter with leaks. The worst case for performance of leaky filters is that penetration over a specific range of flow is proportional to $Q^{-1/2}$. This dependence results in release rate being proportional to $Q^{1/2}$ so that release rate decreases as Q decreases.

The worst situation would be for penetration over some specific range of flows to be inversely proportional to Q to some power greater than 1. This is potentially the case if the observed deviations from filtration theory are not confirmed as being associated with filter leaks. In the flow regions where such a functional dependence on flow exists, release rate would increase as flow decreased. Information on these flow regimes would be critical to manage off-normal releases.

The functional dependence of penetration on flow is being investigated at low flows in this project. The project began in October 1989 with an initial theoretical phase and an experimental phase. The initial theoretical phase was completed in CY 1990 with the derivation of leaky filter behavior at low flows (Scripsick and Hinds, 1990). The experimental phase is ongoing. This summary outlines the results of the initial theoretical phase and describes progress in the experimental phase in CY 1990.

Initial Theoretical Phase

Typically, performance of pleated particulate air filters, made with fibrous media, is extrapolated from fibrous filtration theory for flat sheet media. This approach has been applied in the successful design of fibrous filters for a wide variety of applications, although deviation of filter performance from media performance is well established. Penetration of filters with pinholes differs dramatically from media penetration, especially as flow is lowered. These departures

may be important in applications where filters are used to assure protection of environmental, public, and worker health.

Detailed fibrous filter penetration evaluations in the diffusion collection region (Kozuka, Mikami, and Ikezawa, 1980; Scripsick, 1986; and Hinds and Kraske, 1987) show marked differences when compared with theoretical and experimental evaluations of fibrous media (Liu, Rubow, and Pui, 1985). An example of these differences is shown in Fig. 1. The data of Liu et al. (Liu, Rubow, and Pui, 1985) for high-efficiency particulate air (HEPA) filter media shows characteristics predicted by filtration theory. Scripsick's study (1986) of constructed HEPA filters revealed that penetration maximum disappears and penetration curves cross. These findings suggest that at low filtration velocities filter performance deviates from filtration theory and that penetration in this flow regime may be affected by some size-independent penetration mechanism such as leaks.

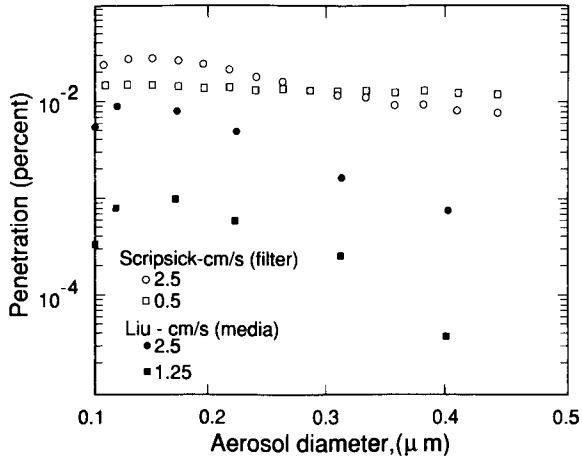

Fig. 1. Penetration data for constructed HEPA filters (Scripsick, 1986) and for HEPA filter media (Liu et al., 1985).

A simple model for predicting performance of a filter with leaks is as follows:

$$P = P_m (1 - Q_L/Q) + Q_L/Q, \qquad (2)$$

where P is overall penetration of the filter, P_m is penetration of the intact media, = exp (-4 α η_{DR} l_f/π d_f), α is the filter media solidity, η_{DR} is the single fiber collection efficiency given by Lee and Liu (1982), l_f is the filter thickness, d_f is effective fiber diameter, Q_L is volume flow through leaks, and Q is the total flow through the filter, which is proportional to Δp, the differential pressure across the filter. When Thomas and Crane (1963) describe performance of filters with leaks, they assumed Q_L was proportional to $Q^{1/2}$. This assumption clearly breaks down at very low values of Q where values of $P > 1$ are predicted. The reason for this failure is that at low Q values, the assumption that Q_L is proportional to $Q^{1/2}$ is no longer valid. The approach in this project phase is to assume that leak flow dependence on Q undergoes a transition from approximately $Q^{1/2}$ to approximately Q, as Q is lowered.

Transition Leak Flow Model

Leak flow is determined by differential pressure and leak geometry. The dependence on these parameters varies with differing leak flow character. The Hagen-Poiseuille equation gives viscous flow in a tube.

$$Q_L = \pi \Delta p\, d^4 / 128\, \mu\, l, \qquad (3)$$

where d is the hole diameter, μ is viscosity, and l is the leak length. Equation 3 shows Q_L to be proportional to Δp. According to Fain (1986), flow through an intact HEPA filter is viscous dominated. Inertial flow in a tube is proportional to Δp to a power <1 but ≥ 0.5.

Kreith and Eisenstadt (1957) provide a method to determine Q_L in the transition between viscous flow and inertial flow. Kreith grouped data into two dimensionless parameters $X = (l/d)\, Re^{-1}$ and $Y = \Delta p/(0.5\, \rho\, U_0^2)$, where Re is the flow Reynolds number, ρ is fluid density, and U_0 is leak flow velocity. To determine Q_L from Δp, l, and d, a plot was made of the dimensionless groups X and $XY^{-1/2}$ (see Fig. 2).

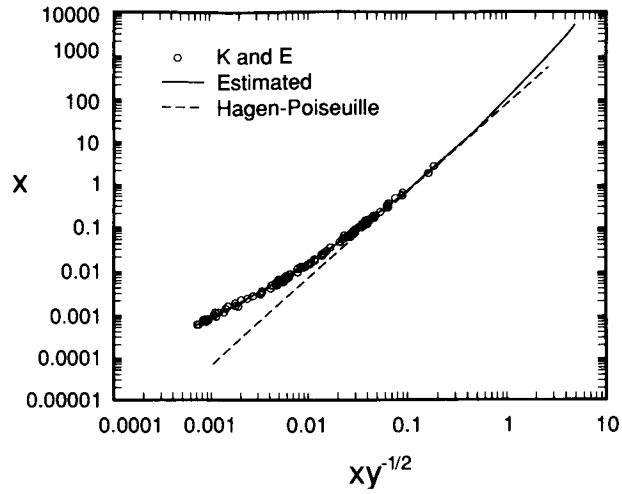

Fig. 2. A plot of X versus $XY^{-1/2}$ showing Kreith and Eisenstadt data (K and E), regression estimates of X, and predictions of the Hagen-Poiseuille equation.

An equation for the curve in Fig. 2 was fit using linear multivariate regression. The fit model was:

$$\text{Log } X = 1.91 + 2.33\, \text{Log}(XY^{-1/2}) + 0.22[\text{Log}^2(XY^{-1/2})]. \qquad (4)$$

Estimates of X from this fit are used to calculate Q_L using the following equation:

$$Q_L = \pi\, l\, \mu / 4\, \rho\, X. \qquad (5)$$

Figure 2 shows at high values of $XY^{-1/2}$, X approaches values predicted by the Hagen-Poiseuille equation and at $XY^{-1/2}$ values >0.08 the fit estimates begin to deviate from the Hagen-Poiseuille predictions. Consequently, Equation 5 is used to predict Q_L for values of $XY^{-1/2}$ from approximately 0.001 to 0.08. For values of $XY^{-1/2} > 0.08$, the Hagen-Poiseuille equation is used to predict Q_L.

Experimental Phase

The overall objective of the experimental phase is to collect data on the performance of fibrous filters operating at low flows. The data to be collected are values of P, Q, and Δp.

Test Stand

In CY 1990, construction of an experimental test stand was completed and most of the test stand proof-testing was completed. We expect to complete proof-testing in the first quarter of CY 1991 and data collection is to be completed by the third quarter of CY 1991.

A diagram of the test stand is shown in Fig. 3. A di-2-ethylhexyl phthalate (Chemical Abstracts Service Number 117-81-7) test aerosol is generated to challenge test filters. Penetration is determined by measuring aerosol concentration upstream and downstream of the test filter. A laser aerosol spectrometer (LAS) is used to make the aerosol concentration measurements as a function of aerosol size. An aerosol diluter was used to reduce the upstream aerosol concentration by a known factor to assure the concentration measured by the LAS is below its upper concentration limit. The LAS is interfaced to a microcomputer for automatic data acquisition. Test filter flow, Q, is measured with a laminar flow element/pressure transducer (LFE/PT) system. Differential pressure across the test filter, Δp, is measured with a micromanometer. Static mixing units are used upstream and downstream of the test filter. The upstream mixer assures a uniform test aerosol challenge over the face of the test filter. The downstream mixer is used to assure that the downstream aerosol concentration sample is representative of the concentration penetrating the test filter.

Proof-Testing

Laboratory proof-testing of specific components of the test stand is required to document their performance. This testing is especially important for the mixing elements. Such elements have had limited application in aerosol studies and their performance has not been rigorously evaluated.

Proof-testing activities completed in CY 1990 include (1) test flow measurement check; (2) system leak check; (3) challenge concentration stability check; (4) upstream mixer/challenge concentration profile; (5) downstream mixer/aerosol loss evaluation; and (6) aerosol diluter calibration.

The LFE/PT system has a certified accuracy of 0.8% of the system reading that is traceable to the National Institute of Standards and Technology (previously the National Bureau of Standards). The accuracy of system readings was checked

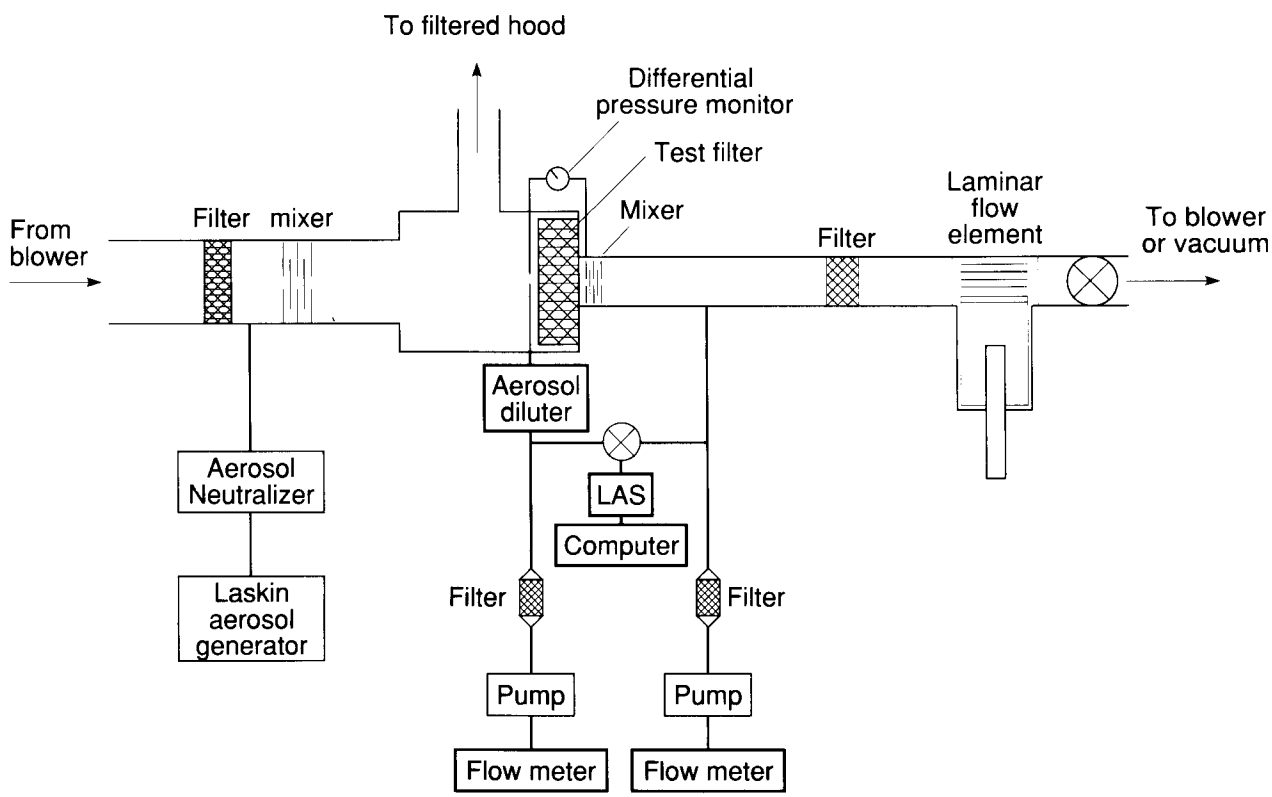

Fig. 3. A diagram of the experimental test stand for measuring penetration at low flows.

with a Gillabrator Bubble Flow Meter in the flow range of approximately 0.03 L/min (LPM) to approximately 20 LPM. The results of this check are shown in Fig. 4. Agreement between the two flow measurement techniques was good except for the extremes of the Gillibrator range of sensitivity.

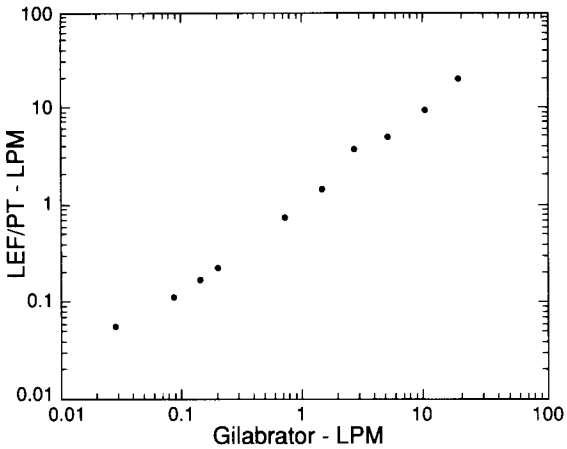

Fig. 4. A plot comparing LFE/PT system flow measurements to Gillabrator measurements.

Test filter flow is provided by maintaining negative pressure downstream of the test filter. Leaks in the negative pressure portion of the test stand can lead to errors in penetration and test flow measurements. This portion of the test stand is tested for leaks by blocking flow to the test filter and putting a 5 in. of H_2O vacuum on the system downstream of the test filter. A 12 LPM flow is circulated through this part of the system and the LAS is used to sample the flow for in-leakage. Under these conditions, on the average less than one particle is detected in 10 min.

Changes in challenge concentration confound measurement of concentration cross-sectional profiles and increase error in filter penetration measurements. Stability of the challenge concentration over time was measured by collecting samples of the challenge with the LAS over long periods of time. At best, the challenge concentration variation was approximately 1%. This variation limits measurement of concentration profile variation to values greater than 1%. The observed stability is sufficient to make filter penetration measurements with the desired precision.

The upstream mixer is used to assure that challenge concentration is uniform over the filter face. The performance of the mixer was evaluated by mapping the concentration profile over the filter face. Variations in challenge concentration with time were accounted for by alternating measurements at grid points on the filter face with measurements at the filter center. The variation observed in the profile measurements was not different fromthe variation observed in the challenge concentration. These data indicate that variability in challenge concentration over the filter face was much less than the time-variation of the challenge.

Aerosol loss in the downstream mixer must be evaluated to make accurate penetration measurements. Losses not accounted for result in underestimation of filter penetration. Aerosol loss evaluations were performed on mixers at their maximum and minimum operation flows. The maximum observed loss was less than 6%.

Dilution ratio is a required factor in the computation of filter penetration. Dilution ratio was determined at four diluter settings over a aerosol diameter range from approximately 0.1 μm to 0.4 μm. These results are shown in Fig. 5. Dilution ratios are observed to be largely independent of aerosol size and approximately equal to values predicted by the Hagen-Poiseuille equation (Eq. 3).

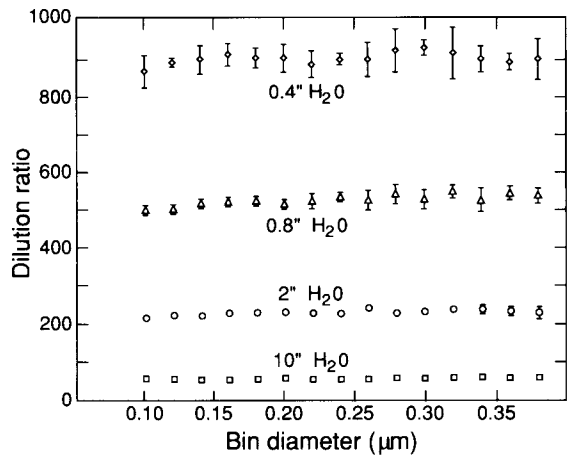

Fig. 5. A plot of dilution ratio versus aerosol size at four diluter differential pressure settings.

Summary

This report summarizes progress in the Low-Flow Filtration project in CY 1990. An initial model of filter performance at low flows was completed. This model assumes that departures from filtration theory are related to filter leaks and that performance at low flow is dominated by leak flow. The model assumes that leak flow undergoes a transition from inertial flow to viscous flow as filter flow drops. In the viscous dominated region, filter penetration is expected to be a constant independent of filter flow.

The experimental phase of the program was initiated in CY 1990. An experimental test stand was completed and much of the proof-testing of the system was finished.

References

Fain, D. A. "Standards for Pressure Drop Testing of Filters as Applied to HEPA Filters," in *Fluid Filtration: Gas, Volume I, ASTM STP 975*, R. R. Raber, Ed., American Society for Testing and Materials, Philadelphia, Pennsylvaniaa (1986).

Hinds, W. C., and G. Kraske. "Performance of Dust Respirators with Facial Seal Leaks: I. Experimental," *Am. Ind. Hyg. Assoc. J.* **48** (10) 836-481 (1987).

Kozuka, M., S. Mikami, and Y. Ikezawa. "Penetrations of High-Efficiency Air Filters for Submicron DOP Aerosol Using a Laser Particle Spectrometer," *VDI-Berichte.* **386**, 23-26 (1980).

Kreith, F., and R. Eisenstadt, "Pressure Drop and Flow Characteristics of Short Capillary Tubes at Low Reynolds Numbers," *Trans. ASME* **79**, 1070 (1957).

Lee, K. W., and B. Y. H Liu. "Theoretical Study of Aerosol Filtration by Fibrous Filters," *Aerosol Science and Technology* **1**, 147-161 (1982).

Liu, B. Y. H., K. L. Rubow, and D. Y. H. Pui. "Performance of HEPA and ULPA Filters," Thirty-First Annual Technical Meeting of the Institute of Environmental Sciences, Las Vegas, Nevada, April 29-May 2, 1985.

Post, D. Statement at meeting on low-flows filtration defining passive safe shutdown (January 10, 1991).

Scripsick, R. C. "New Filter Efficiency Tests Being Developed for the DOE," in *Fluid Filtration: Gas, Volume I. ASTM STP 975*, R. R. Raber, Ed., American Society for Testing and Materials, Philadelphia, Pennsylvania, pp. 345-363. (1986).

Scripsick, R. C., and W. C. Hinds. "Performance of Fibrous Filters at Low Flows" in *Aerosols: Science Industry, Health, and Environment*, S. Masuda and K. Takahashi, Eds. (Pergamon Press, Oxford, 1990) Vol. 2, pp. 821-824.

Thomas, J. W., and G. D. Crane. "Aerosol Penetration through 9-mil HV-70 Filter Paper with and without Pinholes," Eighth Annual AEC Air Cleaning Conference, Oak Ridge National Laboratory, Tennessee, October 22-25, 1963.

Penetrability of Surgical Gloves

Authors: J. F. Stampfer (HSE-5) and R. T. Okinaka (LS-3)
Technical Assistance: R. J. Kissane (HSE-5) and S. M. Schauer (LS-3)
Groups: Industrial Hygiene, HSE-5; Genetics, LS-3
Funding Organization: National Institute for Occupational Safety and Health

Background

As shipped from the manufacturer, many surgical gloves contain small holes. If sufficiently large, these holes markedly degrade protection to infectious agents afforded the wearer. Permeability of surgical and examination-type gloves is of increasing concern with respect to the AIDS human immunodeficiency virus (HIV), which has a diameter of approximately 100 nm, and Hepatitis B with a diameter of 42 nm.

Surgical gloves placed in a saline solution allow a low-voltage current to penetrate, which apparently rises in relation to the length of time the gloves are exposed to the saline solution. As much as 50% of surgical gloves show this electrical permeability, particularly after use.

Test results using various biological agents have been mixed for both surgical and examination-type gloves. Studies of penetrability of gloves that have been used or stretched to small agents have had contradictory results; in no studies did *all* gloves leak or not leak. About 10% of the examination-type gloves that had been stressed and were electrically permeable were also permeable to 1-mm-dia bacteria, while new gloves of this type were impermeable to bacteriophages.

The purpose of this program is to determine whether electrical conductivity is a valid test for the integrity of sterile latex gloves and whether such a test could be employed while the gloves are actually being worn. The relationship between electrical (physical) and viral (biological) penetrability is also investigated. Finally, instruments that measure the electrical permeability and are on the market are evaluated.

Theoretical Base

Theoretical calculations have been performed to determine (1) the sensitivity of the electrical and bacteriophage penetration tests and (2) the smallest sized hole that could be of practical significance.

From simple conduction theory, the current that passes through a hole is given by

$$I = (E/l)A\,\sigma \qquad (1)$$

where:

- E = potential across the material
- l = material thickness
- E/l = potential gradient
- A = hole area = $\pi(d^2/4)$
- d = hole diameter
- σ = specific conductance of conducting solution

Current as a function of hole diameter for a 50-V potential, 0.020-cm-thick material, and 150-g/l NaCl solution is shown in Fig. 1.

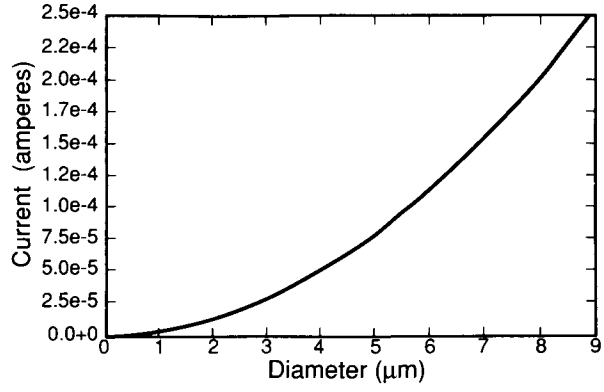

Fig. 1. Current as a function of hole diameter—50-V, 0.020-cm-thick, 140-gal/l NaCl

Concentration or a pressure gradient could cause bacteriophage or HIV particles to penetrate. The number of particles penetrating in a given time caused by a concentration gradient (diffusion) is given by diffusion theory as

$$\text{Number of particles} = -D(T/l)At \qquad (2)$$

where:

- D = diffusion coefficient
- T = titer = concentration of particles in fluid
- l = material thickness
- T/l = concentration gradient
- A = hole area
- t = time

From Equation 2, and assuming a maximum titer of 15000 HIV/cc of fluid, a material thickness of 0.020 cm, and a diffusion coefficient of 4.36×10^{-9} for a 0.1-mm particle, a 145-mm-dia hole would be required for one particle to penetrate in 30 min. We will not consider diffusional penetration further because simpler methods can be used to find large holes, at least before the gloves are donned, such as the water-leak test.

When a pressure difference causes bulk fluid to flow through a hole, the number of particles penetrating is given by the Hagen-Poiseuille equation:

$$\text{Number of Particles} = [(\pi \Delta P d^4)/(128\eta l)]Tt \qquad (3)$$

where:

- ΔP = pressure across hole
- d = diameter of hole
- η = viscosity of fluid
- l = material thickness
- T = titer
- t = time

For the same conditions as used above, a pressure differential of 0.5 atm and a viscosity of .01 poise, a 1.5-μm hole would be required to pass one particle in 30 min. Therefore, particle penetration caused by pressure applied across the material can be important. This pressure is most apt to arise when the wearer tightly grasps an implement. These values are believed to be the maximum amount of time a pressure would be applied at the very spot on the glove where a hole existed. In Fig. 2, we demonstrate that the number of particles penetrating in 30 min under identical conditions decreases rapidly with hole diameter because of the fourth power dependence in Equation 3. Thus we see little point in considering holes smaller than 1 μm.

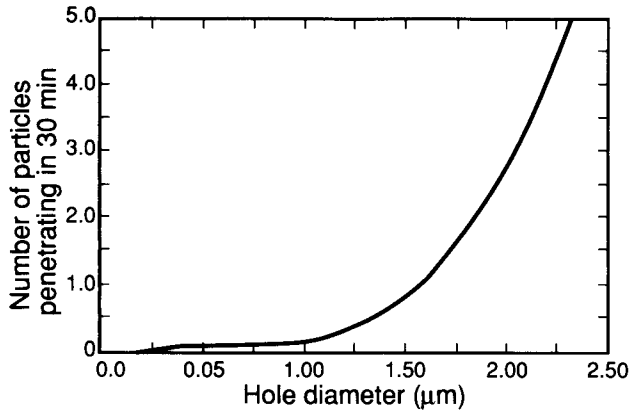

Fig. 2. Number of particles that penetrate decreases with hole diameter.

Figure 3 shows the number of particles that could penetrate a given size hole in 30 min plotted against the current that would flow through that same hole from an applied 50-V potential. Obviously any hole that is large enough to be important will pass an easily measured current, at least at 50 V.

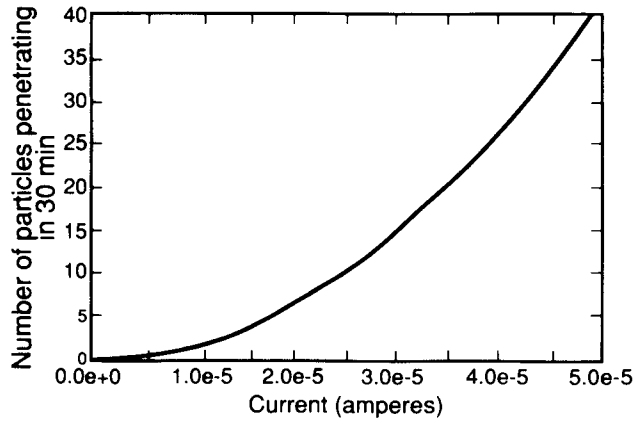

Fig. 3. Number of particles that penetrate a given size hole in 30 min versus current through the same hole.

In testing with bacteriophage, pressure is due to a hydrostatic head of about 15 cm of aqueous bacteriophage solution. A titer as high as 10^7 is used. Phages that penetrate are diluted 80-fold according to experimental protocol. In Fig. 4 we apply this factor of 80 to Equation 3 to show the number of bacteriophages that would be analyzed as a function of hole diameter under these conditions. Again, the number penetrating decreases rapidly with hole size but one could expect one phage to be detected in 30 min if a 2.3-μm hole were present. By increasing the ΦX-174 titer only five-fold, to 5×10^7, a 1.5-μm hole should be detected in 30 min.

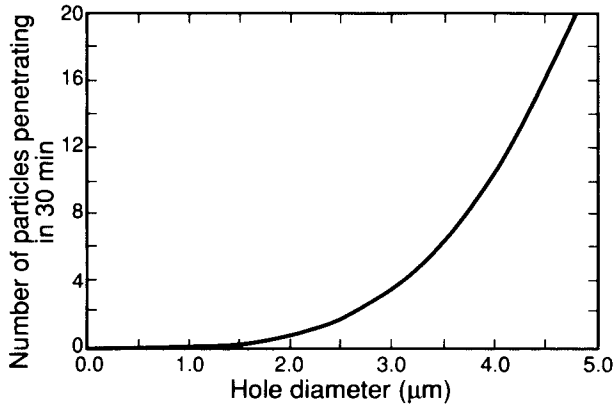

Fig. 4. A factor of 80 applied to Equation 3. Number of penetrating particles analyzed.

In summary, for protection from HIV, the electrical penetration test is more than sensitive enough to detect any hole of importance, and the bacteriophage test can easily be made sensitive enough to locate holes that would be important. Also, it should be possible to compare the results from the two types of tests. One should note that the simple mathematical computations above ignore statistical considerations, which are important when only a few particles are involved, although they are adequate for the range-finding purposes for which they were used.

Results

Physical Penetration. To make the electrical conductivity measurements, a glove is attached to a Teflon ring, which is suspended in a 150-g/L NaCl solution. The same concentration of salt solution is also placed inside the glove. Two platinum electrodes are inserted, one in the glove and the other in the surrounding salt solution; both are attached to a combination power supply and electrometer. A metal ring that is used to hold the glove onto the Teflon ring is also attached to the electrometer and acts as a guard ring to eliminate measuring currents in parallel paths.

The following primary characteristics of a penetration test are shown in Fig. 5: (1) an initial sharp rise in current caused by electrical charging of the glove surfaces; (2) a subsequent decrease as the surfaces approach an equilibrium charge; and finally, (3) a slow increase.

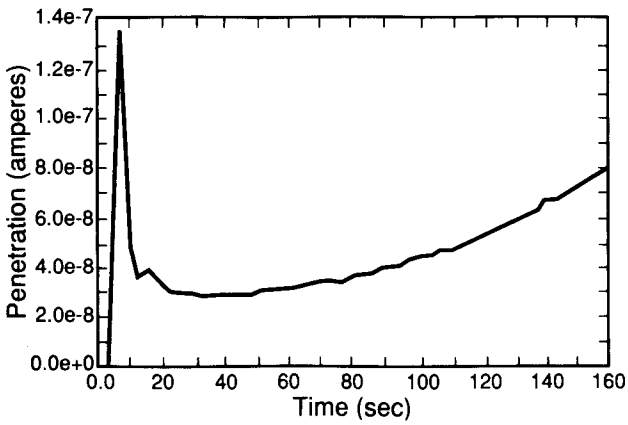

Fig. 5. Primary characteristics of a penetration test.

This final increase is probably caused by a change in the latex material itself and not by any holes that may be present. The data from a 5-hour experiment are shown in Fig. 6. The ordinate scale masks the fact that data at the beginning of the run were similar to other tests. Peaks similar to the one that occurred at approximately 150 min have been recorded in other long-term exposures, although at slightly different times. Also, the total current that had passed through the glove at this time was similar in three out of four experiments, ranging from 0.75° C to 2° C, thus indicating some electrical process within the glove material.

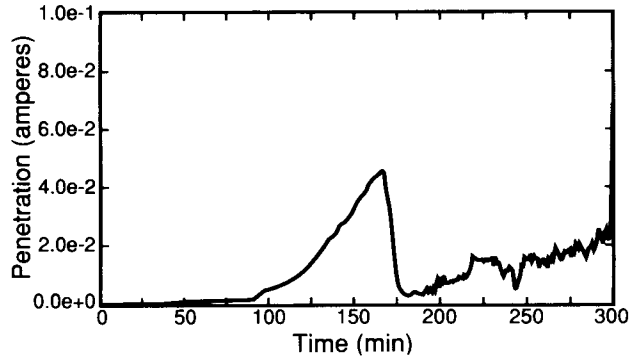

Fig. 6. A 5-hour experiment.

In a number of preliminary experiments, we investigated various aspects and possible problems associated with using electrical conductivity to identify and size holes. One such aspect, time delay, was demonstrated in penetration of glove fingers punctured by a 240-mm acupuncture needle. In some cases more than 5 minutes passed before the holes began to conduct (see Fig. 7). Ten percent of the tests still showed some delay even after we added surfactants to the NaCl solutions.

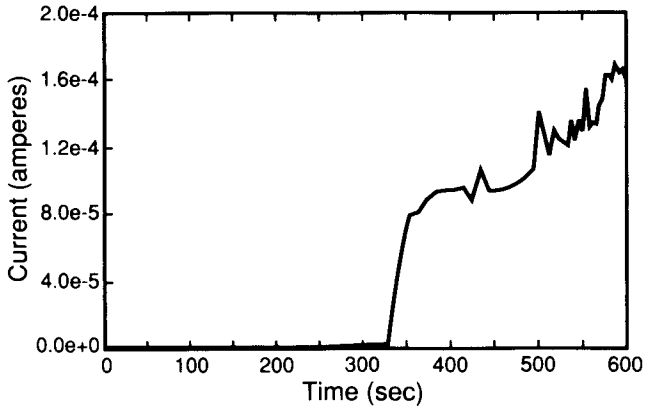

Fig. 7. In some cases more than 5 minutes passed before the holes began to conduct.

This indicates that the problem may be more complex than just the difficulty of the solution's wetting the holes. This is because the surface tension of water, as stated by the manufacturer, becomes constant at 20 dynes/cm and 0.01% surfactant. Perhaps the hole initially closes and then opens again some time after the aqueous solution has contacted the latex. Another possibility is that the presence of the surfactant could change the interaction of the solution with the latex in ways other than simply reducing the surface tension of the solution. And the delay may not occur if measurements are made while the glove is being worn or if the holes are manufacturing defects. However, a sufficiently long delay could indicate that gloves are hole-free when they are not.

Another series of preliminary experiments investigated the effect of pressure on electrical conductivity, an important factor because a glove, when worn, undergoes various pressure changes. As a first attempt at investigating these effects, 30-torr air pressure was applied to the inside of a glove for a specific time and then released. This cycle was repeated a number of times. In the example shown in Fig. 8, pressure was applied at 15 s, 115 s, 215 s, and so on, and released at 65 s, 165 s, 265 s, and so on. When we applied pressure and the glove swelled, causing the latex to thin, penetration *decreased* rather than increased as would be expected. This phenomenon will be investigated further with the gloves restrained. Another experiment will look at penetration changes when the latex is stretched mechanically.

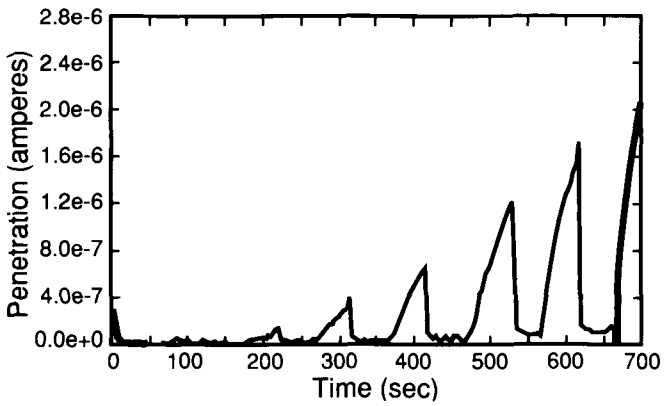

Fig. 8. Pressure was applied at 15 s, 115 s, 215 s, and so on, and released at 65 s, 165 s, 265 s, and so on.

Biological Penetration. The basic protocol for the biological penetration tests has been established, as follows: These tests will be conducted with 27 nm (0.027 μm) ΦX-174 bacteriophage in phosphate-buffered saline (PBS) solutions in concentrations of 1 X 10^6 to 1 X 10^7 phage/cc. The procedure is to fill the glove with the phage solution and then place each glove finger individually into a small container that holds about 40 cc of PBS. The assay consists of inoculating aliquots of an overnight culture of the bacterium *E. coli C*, with dilution of samples from these 40-cc collection containers. The phage-bacteria mixtures are then plated onto a nutrient agar. Following overnight incubation at 37°C, the phage appear as clear circles (plaques) in a "lawn" of bacteria. This technique should reveal penetration volumes as low as 10 nl to be detected.

Development of Models for Carbon Bed Performance

Author: G. O. Wood
Group: Industrial Hygiene, HSE-5
Funding Organization: Department of Energy; Department of Defense

Introduction

Providing respiratory protection is an important contributor to worker safety. Such protection usually takes the form of an air-purifying respirator with cartridges or a canister containing an activated carbon bed through which vapors from solvents or other chemicals are filtered as the worker breathes. Because limited time, funds, or test facilities often preclude extensive testing, these cartridges and canisters are usually qualified for service life after being tested for only one vapor. To ensure cartridge longevity when exposed to several different chemical vapors, researchers in 1990 have been developing models and correlation parameters from which they can estimate the adsorption capacities of activated carbon for a wide range of chemicals.

An important tool in estimating cartridge service life is the adsorption isotherm, a chart that describes, for the material under examination, the effects of vapor concentration on adsorption capacity at a fixed temperature (Fig. 1). To yield an estimate of the respirator's service life, the models described here combine an adsorption isotherm equation, known or easily measured properties of carbon and the vapors of concern, conditions under which the carbon will be required to function as a filter, description of the carbon bed design, and a rate equation.

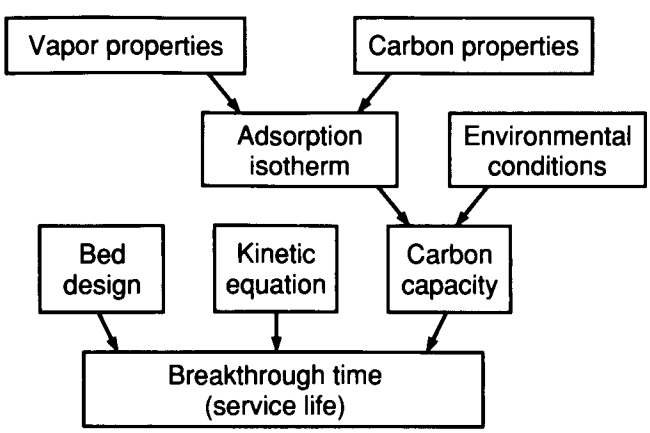

Fig. 1. Breakthrough time determinants for an activated carbon bed.

These models for estimating service life of respirators considered only adsorption as characterized by the reversible and nonreactive interaction of vapors with relatively dry, ordinary activated carbons—those in their original manufactured condition, dried by heating or evacuation, or equilibrated with air at 50% or lower relative humidity. The inclusion of liquid density as an input parameter further limited capacity estimates to those for vapors of organic compounds that exist as liquids at ordinary temperatures and pressures.

Background

Several adsorption isotherm equations have been commonly used to describe the effects of vapor concentration on adsorbed capacity.[1] The Dubinin/Radushkevich (D/R) equation[2] was selected from among these because it has the following desirable characteristics: (1) good data fits, often over wide concentration ranges; (2) inclusion of temperature as a parameter; (3) physical interpretation of parameters; and 4) ease of application.[1] The D/R equation, based on the micropore volume filling theory and the Polanyi concept of adsorption potential and characteristic curves, can be expressed as

$$W_g = W_o\, d_L \exp\{-(KR^2 T^2/\beta^2)\,[\ln(P/P_{sat})]^2\} \quad (1)$$

where

W_g = adsorption capacity (g/g),
W_o = micropore volume (cm^3/g),
d_L = density of condensed liquid in micropores,
T = absolute temperature,
P/P_{sat} = vapor pressure relative to that at saturation,
R = ideal gas constant,
K = carbon structural constant, and
b = affinity (similarity) coefficient.

The carbon structural constant K and the vapor affinity coefficient β appear as a ratio, K/β^2. These parameters are usually separated by using a reference compound, often benzene, for which β is defined as equal to 1.0.[2] Based on experimental measurements of isotherms and derivation of βs, some scientists debate whether reference compounds should

be of similar polarity to those being referenced.[3-5] The use of a reference compound introduces two problems. First, the suspected carcinogenicities of the common capacity reference compounds, benzene and carbon tetrachloride, preclude their routine use. Second, the reference measurement has its own uncertainty, which is often ignored.

Another debate has concerned which parameter β correlates best with molar polarizations, molar liquid volumes, or molecular parchors.[3-5] Researchers have always assumed that β is proportional to one of these measurable properties. Molar polarization is easily calculated for a wide variety of gases and vapors from tabulated physical data or correlations (as shown below); therefore, it was the one chosen for this study.

Affinity Coefficient Correlation

For the first data base, we compiled and calculated 123 values of β^2 from 14 published and unpublished sources.[1,4-16] (We selected the square of β for correlations because it appears in this form in the D/R equation.) Values included were for gas and vapor adsorbates ranging from argon to perchlorocyclopentadiene, including nonpolar, polar, and hydrogen-bonding compounds. First, values for aliphatic acids and amines were excluded as they apparently are unique because of vapor-phase association.[7] Those from questionable data were also excluded: 2,2,4-trimethylpentane,[3] 1,1,2,2-tetrachloroethane,[12] and 2,5-norobornadiene.[8] Any β values based on single isotherm points[4] were not used. First, when reported values were available, they were simply squared.[6-11] In other cases, reported fits of adsorption isotherm data to the D/R equation were used to calculate β^2.[4,14] A third option was to first fit capacity data obtained from reported equilibrium measurements[5,12-13,15] or breakthrough curves[1,16] to the D/R equation. Initially, a reference compound was selected from among those used by each experimenter and a tentative reference value for β^2 was assigned to it. This potential source of bias was later eliminated, as discussed below.

Molar polarizations (P_e, also called molar refraction and proportional-to-electric dipole polarizability) were calculated for each of the compounds for which β^2 values were available. They were calculated using the equation below when a liquid density, a refractive index, n_D, and a molecular weight, M_w, were listed at about 20°C in a handbook:[17]

$$P_e = \frac{n_D^2 - 1}{n_D^2 + 2} \cdot \frac{M^w}{d_L} \qquad (2)$$

When organic compounds were not listed, additive structural contributions were used.[17] A third alternative, used for inorganic gases, was to calculate molar polarizations from tabulated values of polarizabilities by dividing the latter by the conversion constant $0.3964308 \times 10^{-24}$ cm^3.[17]

Figure 2 shows a log-log plot of β^2 versus P_e. The apparent linearity of this plot indicates that β^2 is a power function of P_e. However, because the slope of the plot is less than 2.0, represented by the solid line, the power is less than 2 and β is less than proportional to P_e.

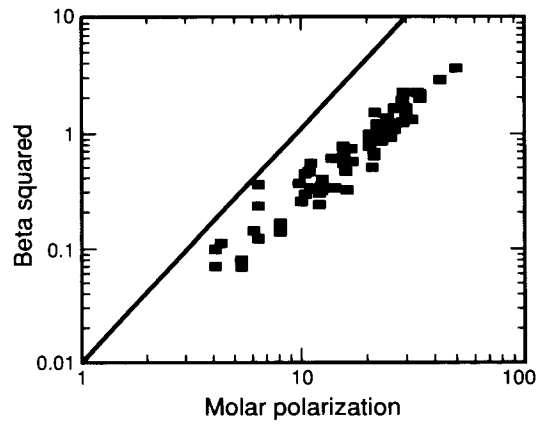

Fig. 2. Affinity coefficient correlation with molar polarization. Straight line slope represents proportionality between b and P_e.

At this point we realized that the value of this slope may be affected by the tentative reference values included in the data. Therefore, an alternate procedure was used for data fitting. Each set of data from the 14 sources was allowed its own "floating" reference value, as follows:

$$\beta^2 = \Sigma_j \, d_{ij} \, a_i \, P_e^{\,m} , \qquad (3)$$

where a_i and m are adjustable curve-fitting parameters and the delta function isolates the data sets i. Nonlinear curve fitting of this equation was done using a commercial program, SYSTAT,* on a PC-compatible 386SX computer. The program produced individual normalization values of a_i for each of the 14 data sets, but a common m, representing the general effect of P_e on β^2, independent of selected reference values of β^2. The value of m that best fit the data (minimum sum of squares of residuals) by this procedure was 1.8. Standard deviation of the 123 β^2 values from this data fit was 0.18. Figure 3 shows the agreement between estimates using this correlation and the experimental β^2 values.

*SYSTAT, Inc., Evanston, Illinois

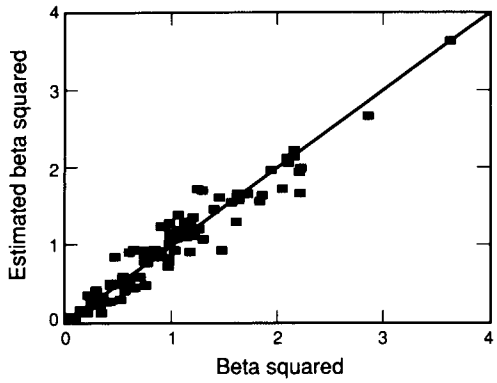

Fig. 3. Comparison of β^2 values estimated by the correlation with experimental β^2 values.

Structural Constant Correlation

The effects of vapor differences on adsorption capacity can be factored out of the K/β^2 ratio using the above correlation, resulting in this form of Equation (1):

$$W_g = W_o\, d_L \exp\{- BP_e^{-1.8} R^2 T^2 [\ln(P/P_{sat})]^2\} \quad (4)$$

where B represents a relative carbon structural constant.

Eighty sets of isotherm data[1,4-5,11-13,15-16,18] were fit to Equation (4) by nonlinear regression using SYSTAT to obtain B and W_o values for each set. These are plotted against one another in Fig. 4.

Figure 4 shows a general trend of increasing B as W_o increases. Such trends have been reported previously for a wide variety of adsorbates, a wide range of temperatures, and two activated carbons.[19] Scatter of the data (also seen in Ref. 19), prohibits precisely defining the relationship between B and W_o; however, it is approximately linear. The scatter in the data may be in part due to the indirect method by which B is determined and sensitivity to experimental errors.

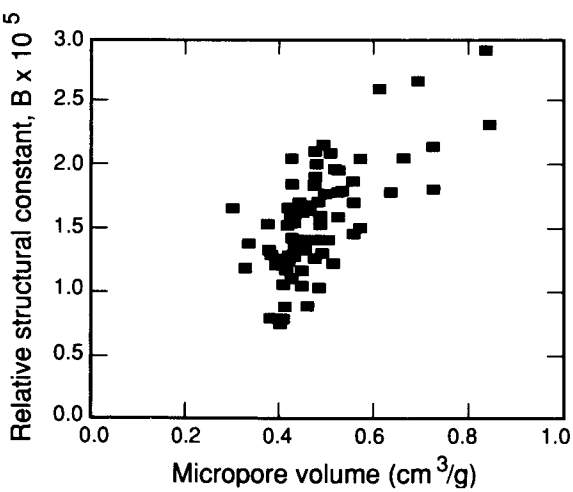

Fig. 4. Relative carbon structural constant versus micropore volume for activated carbons.

Adsorption Isotherm Correlations

A data base was developed containing 1350 capacity data sets from 10 sources[1,4-5,11-13,15-16,18,20] for about 140 different compounds and 15 activated carbons by seven techniques over 20°C-200°C. The data base exclusions were the same as those listed above for affinity coefficient correlations. Aliphatic acids and amines will be considered separately in future work.

With the further assumption that the relative structural constant B is related to micropore volume W_o by the proportionality constant b, Equation (4) becomes

$$W_g = W_o d_L \exp\{- bW_o P_e^{-1.8} R^2 T^2 [\ln(P/P_{sat})]^2\}. \quad (5)$$

Handbook values of liquid density at or near 20°C were used, except for one set of experiments with carbon tetrachloride at 200°C, where the liquid density was taken as 1.19.[18] Saturation vapor pressures at experimental temperatures, easily calculated from tabulated parameters,[21] were used. Molar polarizations were calculated as discussed above. With these inputs, Equation (5) became gravimetric capacity, W_g, as a function of temperature, T, concentration, P, and micropore volume, W_o, with one "universal" constant, b.

All the 1350 data were fit to Equation (5), allowing different adjustable curve fit parameters W_os for each of the 15 carbons, but requiring the same b for all. The value of b that gave the best fit of all the data to Equation (5) was

$$b = 3.56 \times 10^{-5}\ \text{mol}^2\ \text{cal}^{-2}\ \text{cm}_o^{-3}\ (\text{cm}_L^3/\text{mol})^{1.8}, \quad (6)$$

where the subscripts o and L refer to micropore and adsorbate liquid volumes, respectively. The standard deviation of all data from the best fit with 1334 degrees of freedom was 0.029 g/g. Figure 5 shows a comparison of values estimated from the fit with experimental isotherm data. Only eight experimental isotherm data differed from the estimates by more than 0.1 g/g.

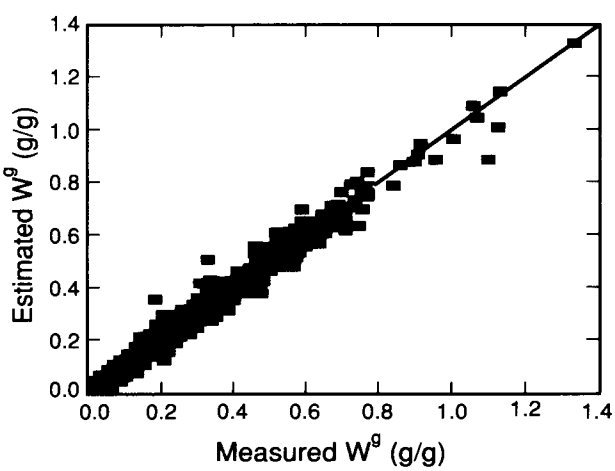

Fig. 5. Comparison of gravimetric capacities estimated by the correlation with experimental capacities.

Sample Application

Assuming a similar activated carbon, Equations (5) and (6) can be used to estimate equilibrium capacities and adsorption isotherms, using only handbook data. For example, assuming a micropore volume of 0.45 cm^3, the capacity for carbon tetrachloride at 840 ppm and 30°C (C_{sat} = 18,7000 ppm for P_{sat} = 142 torr) is estimated to be

$$W_g = (0.45)(1.594)\exp\{-(3.56\times 10^{-5})(0.45)(26.453)^{-1.8}(1.987)^2(303)^2\{\ln(840/187000)\}^2\} = 0.45 \text{ g/g} .$$

This estimate can be improved if the micropore volume can be measured rather than assumed, or if one or more isotherm data can be measured to give a specific b, or both.

Conclusions

Very good adsorption isotherm data correlations were obtained with the D/R equation using only molar polarizations to merge the isotherms for widely different compounds from many different experimental sources. The two most difficult parameters to obtain in the D/R isotherm equation, affinity coefficient and carbon structural constant, have been replaced with molar polarization and a "universal" constant, b. Reference compounds, particularly of differing polarities, were not needed.

Capacities of carbons characterized or qualified with one test vapor can be estimated for other organic vapors using only molar polarizations, liquid densities, and saturation vapor pressures (or concentrations).

References

1. G. O. Wood, and E. S. Moyer, "A Review and Comparison of Adsorption Isotherm Equations Used to Correlate and Predict Organic Vapor Canister Capacities," *Am. Ind. Hyg. Assoc. J.* **52**, *235-242 (*1991).
2. M. M. Dubinin, in *Progress in Surface Membrane Science*, Vol. 9, D. A. Cadenhead, J. F. Danielli, and M. D. Rosenberg, Eds. (Academic Press, New York, 1975).
3. P. J. Reucroft, W. H. Simpson, and L. A. Jonas, *J. Phys. Chem.* **75**, 3526 (1971).
4. A. Golovoy and J. Braslaw, *J.A.P.C.A.* **31**, 861 (1981).
5. K. E. Noll, D. Wang, and T. Shen, *Carbon* **27**, 239 (1989).
6. M. M. Dubinin, in *Chemistry and Physics of Carbon*, Vol. 2, P. L. Walker, Ed. (Marcel Dekker, New York, 1966), p. 1.
7. M. M. Dubinin and D. P. Tomofeyev, *C. R. Acad. Sci. URSS* **54**, 701 (1946).
8. F. Kraehenbuehl, H. F. Stoeckli, A. Addoun, P. Ehrburger, and J. B. Donnet, *Carbon* **24**, 483 (1986).
9. O. Kadlec, *Chem. Pap.* **29**, 660 (Slovak Academy of Sciences, Bratislava, 1975).
10. H. F. Stoeckli and D. Morel, *Chemia* **34**, 502 (1980).
11. K. Urano, S. Omori, and E. Yamamoto, *Environ. Sci. Technol.* **16**, 10 (1982).
12. W. H. Simpson, P. J. Reucroft, and P. J. Hackett, "Sorption Properties of Activated Carbon," Franklin Institute Research Laboratories report F-C2587 (1970).
13. P. J. Reucroft, H. K. Patel, W. C. Russell, and W. M. Kim, "Modeling of Equilibrium Gas Adsorption for Multicomponent Vapor Mixtures, Part II," US Army Chemical Research, Development, and Engineering Center report CRDEC-CR-87015, Aberdeen Proving Ground, Maryland (1986).
    Additional data provided in private communication from P. J. Reucroft (1989).
14. J. J. Hacskaylo and M. D. LeVan, *Langmuir* **1**, 97 (1985).
15. E. D. Tolles, J. C. Mullins, and J. K. Evans, "Sorption Properties of Activated Carbon," US Army report AD-860466, Aberdeen Proving Ground, Maryland (1969).
16. G. O. Nelson and C. A. Harder, *Amer. Ind. Hyg. Assoc. J.* **37**, 205 (1976).
    Extensive breakthrough curve data at various concentrations were provided by private communication, 1988.
17. *CRC Handbook of Chemistry and Physics*, 67th Ed., R. C. Weast, Ed. (CRC Press, Inc., Boca Raton, Florida 1987).
18. D. Trout, P. N. Breysse, T. Hall, M. Corn, and T. Risby, *Am. Ind. Hyg. Assoc. J.* **47**, 491 (1986).
19. H. F. Stoeckli and J. Ph. Houriet, *Carbon* **14**, 253-256 (1976).
20. G. O. Nelson, and C. A. Harder, *Amer. Ind. Hyg. Assoc. J.* **35**, 391 (1974).
21. R. C. Reid, J. M. Prausnitz, and T. K. Sherwood, *The Properties of Gases and Liquids*, Third Edition (McGraw-Hill Book Co., New York, 1977).

Solid Phase Extraction System

Author: Peter Del Mar, HSE-9
Group: Health and Environmental Chemistry
Funding Organization: Department of Energy

We sought to determine if the solid phase extractor and methodology currently useful for pesticide extractions is useful for semivolatile extractions. This approach has already been shown to be technically feasible and had been reduced to a practical, operational device.

The novel feature in our approach was the use of relatively large-bore plastic tubing to separate organic compounds from water in contrast to former use of packed beds of sorbent material or even older solvent extraction methods. Present Environmental Protection Agency (EPA) methods for extracting organic target compounds from water samples are extremely time consuming, use large amounts of solvents, and give results that are prone to error and bias.

The success of the new method is based on its simplicity. This extractor uses 1.0-mm-i.d. plastic tubing to collect pollutants from water. Following the separation, a small amount of solvent is used to recollect the pollutants of interest. The extract is then analyzed using current EPA methods. By using open tubes as sorbent surface, we developed a system that is durable, indefinitely reusable, fast, and easy to use. We have also been able to achieve a precision and accuracy at least ten times better than reported by other laboratories using currently accepted solvent extraction techniques. These results are based on participation in EPA water studies involving several hundred laboratories nationwide.

A prototype 10-channel separator has been built and its performance validated by successful analysis of EPA pesticide performance samples as part of the EPA water pollution and water supply performance evaluation programs. New specially made tubing without plasticizers is currently being evaluated.

Among the gains already realized in developing our open tubular solid phase method are reducing sample preparation times by 75%, providing more precise and accurate analysis, reducing handling, and minimizing waste. The new technology also reduces by 90% the use of solvents that themselves become harzardous wastes. And it eliminates the automatic contamination by extraction solvent during radioactive sampling. Experimental work has now shown that polychlorinated biphenyls as well as pesticides can be analyzed using this technique. The new technology provides a more cost-effective way of meeting the new EPA Land Ban requirements involving the toxicity characteristic leaching procedure. In addition to its role in environmental compliance activities at LANL, the technique can be transferred to the private sector for use in all applicable chemical analyses in support of environmental programs.

Because we have identified all the significant sources of variability in the method, project objectives are now focused in two specific areas:

- better material for columns to enable us to recover more target compounds and lower detection limits
- extending the technique to as many different lists of target compounds as possible

Our present goal is to broaden our understanding of the actual extraction mechanism and to obtain better materials so that a second, more advanced prototype can be built for transfer to an industrial partner.

Health and Environmental Chemistry

Distribution of Plutonium and Americium in Whole Bodies Donated to the United States Transuranium Registry

Authors: J. F. McInroy, J. J. Miglio, E. R. Gonzales, L. C. Willis, K. Jarrett, R. L. Kathren,* and Margery J. Swint*
Groups: Health and Environmental Chemistry (HSE-9), *Hanford Environmental Health Foundation, Richland, Washington
Funding Organizations: Department of Energy, Office of Environmental Health, HHS, National Cancer Institute

Radiochemical analyses of whole body donations from six former nuclear industry workers 30 or more years after exposure have been completed. One individual had been exposed to americium-241 only. The others had primarily been exposured to plutonium, but small quantities of americium were also present in their tissues.

The plutonium-239 and americium-241 content of each specific tissue or organ for each whole body case, expressed in terms of the percentage of the total activity in the whole body for each specific tissue or organ, are found in the Tables I-VI. Complete analytical data have not been reproduced, but the results provided are sufficient to estimate the whole body distribution of plutonium-239 from five cases and the distribution of americium-241 for four and to make a preliminary evaluation of these data in terms of existing biokinetic models. The systemic (excluding the lungs) plutonium-239 activity measured in the tissues is compared with the deposition estimated *in vivo* in Table VII. In general, the estimated activity based on *in vivo* measurements is several times greater than the measured postmortem activity in the tissues. These results are in excellent agreement with the recent study by Kathren, Heid and Swint[1] in which *in vivo* estimates of systemic deposition were compared with estimates made from postmortem analyses of selected tissues. This comparison showed an inverse relationship between the measured activity in the tissues and the ratio of *in vivo* to postmortem estimates of systemic deposition.

The distributions of plutonium-239 and americium-241, expressed as a percentage of the total body content or of the systemic deposition, are given in Tables VIII-XI. For those cases in which inhalation was the primary route of entry, a large fraction of the total body burden was found in the respiratory tract. This does not appear consistent with the current International Commission on Radiological Protection (ICRP) lung model[1,2] that predicts a smaller fraction of actinide to be retained in the respiratory tract.

By comparison, the distributions of plutonium-239 and americium-241 differ. For both nuclides, a greater fraction of the total body burden is found in the soft tissues, in particular the muscle, than inferred from the models proposed in ICRP Publications 30 and 48.[2,3] For plutonium-239 the distribution in skeleton and liver (Table XII) is more consistent with the initial equal fractionation of this nuclide between skeleton and liver proposed in ICRP Publication 30. The overall systemic distribution of plutonium-239 is well characterized by using ICRP 30 parameters for initial fractionation and half-life in skeleton and liver, assuming that all or at least a portion of the remainder in the transfer compartment is deposited in the remaining soft tissues with a long half-life (Table XII).

For americium-241, the systemic distributions observed in these cases are more consistent with the 50:30 fractionation between skeleton and liver proposed in ICRP Publication 48, and an effective clearance half-time of about 2 years for americium-241 in the liver as was proposed by Durbin and Schmidt[4] based on their analysis of Case 102, and by Griffith and coworkers[5] from animal data. The observed distributions are also consistent, as is the fractionation of plutonium discussed above, with the observations of Kathren *et al*[6] on long-term exposure cases from which selected tissues had been obtained, and with the preliminary analysis of Case 193 previously reported by McInroy *et al.*[7]

Table I. Distribution of americium-241 in USTR Case No. 102 (plutonium-239 data not available).

		Americium-241 retention	
Tissue/organ	**Wet weight (g)**	**Activity (Bq)**	**Distribution (percent)**
Respiratory tract	2 521	82.9	1.55
Liver	1 450	344.8	6.44
Kidneys	250	13.3	0.25
Spleen	145	3.4	0.06
Smooth muscle organs	990	28.1	0.52
Striated muscle and skin	23 909	469.9	8.78
Other tissue	86	4.1	0.08
Testes	26	0.2	0.004
Bones and teeth (ash weight 2 539 g)	8 992	4 406.7	82.36
Total whole body	**38 366**	**5 350.2**	**100.0**

Table II. Distribution of plutonium-239 and americium-241 in USTR Case No. 193.

Tissue/organ	Wet weight (g)	Plutonium-239 retention Acitivity (Bq)	Plutonium-239 retention Distribution (percent)	Americium-241 retention Activity (Bq)	Americium-241 retention Distribution (percent)
Respiratory tract	1 337	130.0	52.75	16.28	60.70
Liver	1 863	48.6	19.74	1.42	5.29
Kidneys	326	0.1	0.03	0.01	0.03
Spleen	258	1.5	0.59	0.10	0.46
Smooth muscle organs	1 972	0.6	0.24	0.14	0.53
Striated muscle	24 659	8.6	3.48	1.82	6.80
Other muscle	968	0.3	0.12	0.03	0.11
Skin	19 688	2.6	1.06	0.49	1.82
Other soft tissue	1 806	3.0	1.23	0.39	1.45
Testes	14	0.0	0.00	0.00	0.01
Bones and teeth (ash weight 2 681 g)	8 691	51.1	20.76	6.15	22.93
Totai whole body	**61 583**	**246.4**	**100.00**	**26.82**	**100.00**

Table III. Distribution of plutonium-239 and americium-241 in USTR Case No. 208.

Tissue/organ	Wet weight (g)	Plutonium-239 retention Acitivlty (Bq)	Plutonium-239 retention Distribution (percent)	Americium-241 retention Activity (Bq)	Americium-241 retention Distribution (percent)
Respiratory tract	972	85.6	37.75	2.08	28.89
Liver	1 600	35.7	15.74	0.16	2.23
Kidneys	375	0.2	0.07	0.01	0.13
Spleen	104	0.1	0.04	0.02	0.26
Smooth muscle organs	2 699	0.8	0.35	0.03	0.48
Striated muscle	24 686	12.8	5.64	1.21	16.83
Other muscle	1 111	0.8	0.37	0.03	0.44
Skin	7 082	1.4	0.61	0.09	1.20
Other soft tissue	1 355	1.0	0.42	0.05	0.72
Testes	29	0.07	0.03	0.004	0.06
Bones and teeth (ash weight 2600 g)	8 407	88.4	38.97	3.50	48.76
Total whole body	**49 420**	**226.7**	**100.00**	**7.18**	**100.00**

Table IV. Distribution of plutonium-239 and americium-241 in USTR Case No. 213.

Tissue/organ	Wet weight (g)	Piutonium-239 retention Acitivlty (Bq)	Piutonium-239 retention Distrlb-ution (percent)	Americlum-241 retention Activity (Bq)	Americlum-241 retention Distrib-ution (percent)
Respiratory tract	1 698	56.3	18.57	2.54	14.73
Liver	2 604	47.8	15.77	0.42	2.46
Kidneys	670	0.5	0.16	0.02	0.14
Spleen	236	1.6	0.53	0.02	0.12
Smooth muscle organs	2 518	1.3	0.43	0.10	0.57
Striated muscle	23 930	12.3	4.06	1.08	6.26
Other muscle	835	0.8	0.27	0.04	0.25
Skin	12 720	3.9	1.27	0.55	3.19
Other soft tissue	2 071	3.9	1.28	0.19	1.08
Testes	38	0.2	0.05	0.001	0.01
Bones and teeth (ash weight 2 850 g)	9 084	174.8	57.61	12.29	71.17
Total whole body	**56 403**	**303.3**	**100.00**	**17.26**	**100.00**

Table V. Distribution of plutonium-239 in USTR Case No. 212 (americium-241 data not available).

Tissue/organ	Wet weight (g)	Americium-241 retention Activity (Bq)	Americium-241 retention Distribution (percent)
Respiratory tract	1 698	0.8	0.36
Liver	2 382	85.7	41.09
Kidneys	461	0.2	0.08
Spleen	243	0.3	0.16
Smooth muscle organs	594	0.03	0.02
Striated muscle	27 735	13.9	6.65
Other muscle	618	0.2	0.08
Skin	23 650	4.8	2.29
Other soft tissue	2 104	0.3	0.16
Testes	61	0.1	0.04
Bones and teeth (ash weight 2 998 g)	10 704	102.3	49.08
Total whole body	**70 247**	**208.5**	**100.0**

Table VI. Distribution of plutonium-239 in USTR Case No. 242 (americium-241 data not available).

Tissue/organ	Wet weight (g)	Plutonium retention: Activity (Bq)	Plutonium retention: Distribution (percent)
Respiratory tract	1 207	1 861.7	65.65
Liver	1 620	390.4	13.79
Kidneys	312	0.5	0.02
Spleen	205	11.8	0.42
Smooth muscle organs	262	0.2	0.01
Striated muscle	36 690	34.2	1.21
Other muscle	677	5.3	0.19
Skin	20 085	12.1	0.43
Other soft tissue	4 979	132.9	4.69
Testes	24	0.1	<0.01
Bones and teeth[2] (ash weight 3 069 g)	10 026	3 384.9	13.60
Total whole body	**75 703**	**2791**	**100.0**

Table VII. Comparison of systemic plutonium-239 estimates made *in vivo* with postmortem tissue analysis results.

USTR Case No.	*In vivo* estimate	Systemic plutonium-239 (Bq) postmortem measurement	Ratio, *in vivo* to postmortem
193	995	116	8.6
208	574	141	4.1
212	535	209	2.6
213	585	247	2.4
242	925	972	1.0

Table VIII. Distribuiton of plutonium-239 in five whole bodies (percent whole body content).

USTR Case No.	Likely route of entry	Respiratory tract	Liver	Skeleton	Muscle	Other
193	inhalation	52.8	19.7	20.8	3.5	3.3
208	inhalation	37.8	15.7	39.0	5.6	1.9
212	wound	0.4	41.1	49.1	6.6	2.8
213	inhalation	18.6	15.8	57.6	4.1	4.0
242	inhalation	**65.6**	**13.8**	**13.6**	**1.4**	**4.7**
Mean, all cases (N = 5)		35.1	21.2	36.0	4.2	3.3
Standard deviation		26.2	11.3	18.6	2.0	1.1
Mean, inhalation cases only (N = 4)		43.8	16.2	32.8	3.7	3.5
Standard deviation		20.3	2.5	19.7	1.7	1.2

Table IX. Distribution of plutonium-239 in five whole bodies (percent systemic content).

USTR Case No.	Liver	Skeleton	Muscle	Other
193	41.8	43.9	7.4	7.0
208	25.3	62.6	9.1	3.0
212	41.3	49.2	6.7	2.8
213	19.4	70.8	5.0	4.9
242	40.1	39.6	4.1	16.2
Mean	33.6	53.2	6.7	6.8
SD*	10.5	13.1	1.8	5.5

*Standard deviation.

Table X. Distribution of americium-241 in four whole bodies (percent whole body content).

USTR Case No.	Likely route of entry	Respiratory tract	Liver	Skeleton	Muscle	Other
102	wound	1.5	6.4	82.4	8.8	0.9
193	inhalation	60.7	5.3	22.9	6.8	4.3
208	inhalation	28.9	2.2	48.8	16.8	3.3
213	inhalation	14.7	2.5	71.2	6.3	5.3
Mean, all cases (N=4)		26.4	4.1	56.3	9.7	3.4
Standard deviation		25.4	2.1	26.3	4.9	1.9
Mean, inhalation cases only (N = 3)		34.8	3.3	47.6	10.0	4.3
Standard deviation		23.6	1.7	24.2	5.9	1.0

Table XI. Distribution of americium-241 in four whole bodies (percent systemic content).

USTR Case no.	Liver	Skeleton	Muscle	Other
102	6.5	83.7	8.9	0.9
193	13.4	58.3	17.3	10.9
208	3.3	68.6	23.7	4.4
213	2.9	83.5	7.4	6.3
Mean	6.5	73.5	14.3	6.6
SD*	4.8	12.4	7.6	4.2

*Standard deviation.

Table XII. Percentage of systemic activity 30 years after exposure.

	Mean ± of 5 cases, this study	ICRP Parameters[a]	ICRP 48 Case I[b]	ICRP 48 Case II[c]
Skeleton	53.7 ± 12.5	50	52	52
Liver	35.4 ± 12.5	36	16	12
Remainder of body	10.9 ± 2.1	14	20	33

[a]Assumes initial partitioning of 0.45 to skeleton, 0.45 to liver, and 0.10 to remainder of body and early excretion; retention half-times of 100 years in skeleton and 40 in liver.[2] Of portion not going to skeleton or liver, half is assumed to be excreted rapidly and half deposits in other tissues with essentially infinite half-life.
[b]Assumes initial partitioning of 0.50 to skeleton; 0.30 to liver, and 0.20 to remainder of body and early excretion; retention half-times of 100 years skeleton and 50 years in liver;[3] other assumptions as in table note a, above.
[c]Assumptions as for table note b except retention half-times of 50 years in skeleton and 20 years in liver.
Activity calculation:

$$\%\ \text{activity at time t in compartment i} = \frac{f_i e^{-\lambda_i t}}{\Sigma f_i e^{-\lambda_i t}} \times 100\%$$

where f_i is the fraction initially deposited in organ i, λ_i is the effective removal constant from organ i, and t is the time deposition.

Conclusions

Radiochemical analysis of whole body donations from six former nuclear industry workers 30 or more years after exposure revealed about 44% of the total body deposition of plutonium-239 and 35% of the americium-241 were found in the respiratory tract of the four cases with inhalation exposure. These proportions are greater than predicted by the current ICRP lung model.

Exclusive of the respiratory tract, the mean fractional systemic deposition of plutonium-239 in the tissues of five whole bodies consisted of the following: liver 33.6 ± 10.5%; skeleton 53.2% ± 13.1%; striated muscle 6.7% ± 1.8% and all other organs and tissues6.8% ± 5.5%. For americium-241, the comparable values in four cases were liver 6.5% ± 4.8%; skeleton 73.5% ± 12.4%; muscle 14.3% ± 7.6%; and all other tissues and organs 6.6% ± 4.2%. The systemic distribution of plutonium-239 was generally consistent with ICRP Publication 30. A significant fraction of both nuclides was retained in the muscle and other soft tissues that serve as long-term storage depots. Initial fractionation of americium-241 between skeleton and liver is consistent with the 50:30 ratio proposed in ICRP Publication 48 with an effective clearance half-time from the liver of about 2 years. Estimates of plutonium-239 deposition made on the basis of urinalysis results *in vivo* were typically greater than the observed deposition measured in the tissues of the whole body after death.

Although it should be stressed that the data evaluations presented here are only preliminary, there appear to be clear differences between the recent ICRP biokinetic models for Pu and Am and the results in these six whole bodies, leading to the following tentative conclusions:

For the inhalation exposure cases, greater proportions of plutonium-239 and americium-241 are found in the respiratory tract than would be predicted by the ICRP lung model.[2] This suggests that retention fractions and retention half-times in the respiratory tract may be greater than proposed by the ICRP lung model.

In general, systemic distribution of plutonium-239 is reasonably well characterized by the model in ICRP Publication 30.[2] Initial fractionation of plutonium-239 between liver and skeleton is approximately equal and consistent with the values specified in ICRP Publication 30.

Initial fractionation of americium-241 between liver and skeleton is consistent with the 50:30 ratio cited in ICRP Publication 48 and with a clearance half-time from the liver of about 2 years.

After a long-term exposure, significant fractions of the systemic plutonium-239 and americium-241 are found in the muscle and other soft tissues, suggesting that these tissues represent a long-term depot for these nuclides.

In vivo estimates of systemic deposition typically are several times greater than the deposition measured in the tissues of the whole body after death. This confirms observations from prior studies using tissue samples only and suggests that *in vivo* estimates made from commonly used biokinetic models may greatly exaggerate the actual deposition.

Study and evaluation of these cases, as well as the results from partial body autopsy cases is continuing, and additional and more detailed reports are anticipated.

References

1. R. L. Kathren, K. R. Heid, and M. J. Swint, "Comparison of Estimates of Systemic Pu from Urinary Excretion with Estimates from Postmortem Tissue Analysis," *Health Phys.* **53**, 487-494 (1987).
2. "Limits for Intakes of Radionuclides by Workers," ICRP **30** (Pergamon Press, Oxford, 1979).
3. "The Metabolism of Plutonium and Related Elements," *ICRP* **48** (Pergamon Press, Oxford, 1986).
4. P. W. Durbin, and C. T.Schmidt, "The U. S. Transuranium Registry Report on the ^{241}Am Content of a Whole Body. Part V: Implications for Metabolic Modelling," *Health Phys.* **49**, 623-661 (1985).
5. W. C. Griffith, J. A. Mehwhinney, B. B. Muggenburg, B. B. Boecker, and R. G. Cuddihy, "Bioassay Model for Estimating Body Burdens of ^{241}Am from Excretion Analysis," *Health Phys.* **44** (Suppl. 1), 545-554 (1983).
6. R. L. Kathren, J. F. McInroy, M. M. Reichert, and M. J. Swint, "Partitioning of ^{238}Pu, ^{239}Pu and ^{241}Am in Skeleton and Liver of U. S. Transuranium Registry Autopsy Cases," *Health Phys.* **54**, 181-188 (1988).
7. J. F. McInroy, R. L. Kathren, G. L. Voelz, and M. J. Swint, "U.S. Transuranium Registry Report on the Pu-239 Distribution in a Human Body," *Health Phys.* **52** (Suppl. 1), S37 (1987).

Environmental Chemistry for the National Park Service

Authors: E. S. Gladney[1] and R. W. Ferenbaugh[2]
Groups: [1]Health and Environmental Chemistry (HSE-9), [2]Environmental Protection (HSE-8)
Funding Organizations: Air Quality Division, National Park Service

Through an Interagency Agreement with the Air Quality Division of the National Park Service, Los Alamos National Laboratory has assessed the effects of air pollution at selected national parks and monuments, including Arches National Park, Bandelier National Monument, Canyonlands National Park, Cascades National Park, Chaco Culture Natural History Park, Chiricahua National Monument, Everglades National Park, Mesa Verde National Park, Petrified Forest National Park, Saguaro National Monument, and Walnut Canyon National Monument. Los Alamos researchers have undertaken the following projects.

Sulfur Dioxide Fumigation of Piñon Pine Seeds and Seedlings. These studies were designed to determine the effects of sulfur dioxide, a common pollutant from power plants and smelters, on the tree species *Pinus cembroides* in Southwestern parks and monuments. Researchers performed both acute and chronic fumigations on piñon pine seeds and seedlings. Although the final statistical analysis is not complete, preliminary indications are that piñon pine is resistant to sulfur dioxide, showing detrimental fumigation effects only at high ambient sulfur dioxide concentrations.

Baseline Sulfur Concentrations around Four Corners. To provide a baseline against which to assess effects of power plant emissions, Los Alamos researchers measured the sulfur content of foliage and soil samples from five parks and monuments around the Four Corners power plant. They are comparing sulfur concentrations from the five parks and monuments, both among the parks and monuments and from within each park or monument. Samples from different soil depths and from different year classes of needles are also being compared. Preliminary indications from these comparisons are that the source of variability differs from park to park.

Saguaro National Monument. Researchers investigated a possible association between the "saguaro decline" and air pollution. They analyzed tree cores, samples of saguaro tissue, and soils from both within and outside the monument for metals. Data compiled to date indicate no trends that can be linked to the decline.

Everglades National Park. Los Alamos staff analyzed metals in pine needle samples from Everglades National Park and provided data for interpretation by the National Park Service.

Cascades National Park. Researchers seeking to provide baseline data and to assess smelter emission impact upon the park gathered samples of subalpine fir needles, lichens, and soils from Cascades National Park. They then analyzed the samples for metals and are now performing statistical analysis on the data.

Rock Pool Study. Researchers began analyzing water chemistry on samples taken from natural rock pools in Canyonlands and Arches National Parks to determine if the pools are being affected by pollutant emissions. Preliminary evaluation of the data indicates no discernable impacts.

Cryptogamic Soil Study. Samples of cryptogamic soils from several national parks and monuments on the Colorado Plateau are being analyzed to investigate pollutant impact on these soils. Sample analysis for this study is still under way.

Occupational Medicine

Mortality among 241 Los Alamos Plutonium Workers

Authors: Laurie D. Wiggs, George L. Voelz, and Emily R. Johnson
Group: Occupational Medicine, HSE-2
Funding Organization: DOE, Office of Health and Environmental Research

In 1974, Los Alamos researchers identified a group of 241 workers having the highest plutonium body burdens. These workers, 224 white males and 17 white females, had estimated body burdens of at least 10 nCi, which represents 25% of the maximum permissible body burden for Pu.[1] Dose estimates have been revised downward for many of these workers since the initial study selection. Nevertheless, these workers still represent the more highly plutonium-exposed workers at Los Alamos.

Mortality through 1980 for these workers has been reported.[1] As of 1980, there had been 43 deaths among the males and 3 among the females. Mortality among the males was 56% of deaths expected from all causes combined and 54% of deaths expected from all malignant neoplasms.

In 1990, we updated the follow-up for these workers and reexamined their mortality patterns. Through the end of 1989, 77 males and 5 females had died. Mortality among the males is still significantly less than that expected, based on US death rates, with mortality from all causes at 62% of expected and mortality from all cancers at 64% of expected. Table I presents standardized mortality ratios (SMRs) for the white males through the end-of-study date of December 31, 1989.

Among the females in the group, two of the five deaths were due to cancer. The SMR for all causes of death among these females was 75 (95% confidence interval [C. I.]) 24 - 176 and the SMR for all cancers was 115 (95% C. I. 13 - 414). The two observed cancer deaths were from cancer of the gallbladder and cancer of the brain.

Table I. Mortality among 224 Los Alamos National Laboratory white male plutonium workers

	Observed	Expected	SMR	95% C.I.
All causes of death	77	124.7	62	49 - 77
All cancers	18	28.2	64	38 - 101
Oral cancers	1	0.8	124	02 - 692
All digestive cancers	5	7.4	67	22 - 157
Lung cancers	5	9.8	51	17 - 120
Prostate cancers	2	2.1	97	11 - 351
Bladder cancers	1	0.8	128	02 - 715
Brain cancers	1	0.8	131	02 - 732
Lymphosarcomas	1	0.5	224	03 -1247
All circulatory diseases	31	63.3	49	33 - 70
All respiratory diseases	8	8.5	94	41 - 186
All injuries	10	9.2	109	52 - 200

References

1 G. L. Voelz, G. S. Wilkinson, J. W. Healy, J. F. McInroy, and G. L. Tietjen, "Mortality Study of Los Alamos Workers with Higher Exposures to Plutonium," in *Epidemiology Applied to Health Physics, Proceedings of the Sixteenth Midyear Topical Meeting of the*

Mortality among White Males Employed by the Los Alamos National Laboratory from 1943-1977

Authors: Laurie D. Wiggs, Carol Cox -DeVore, and George L. Voelz
Group: Occupational Medicine, HSE-2
Funding Organization: Department of Energy: Office of Health and Environmental Research

Analyses examining mortality among white males employed by the Los Alamos National Laboratory from 1943 through the end of 1977 are currently under way. The study cohort includes 15,726 white males who were followed an average of 22.2 years as of the end-of-study date (EOS) of December 31, 1983.

Results of preliminary standardized mortality analyses are presented in Table I. There were 2182 deaths recorded in the cohort as of the EOS, 482 of which were attributed to some type of cancer. The standardized mortality ratio (SMR) for all causes of death indicates that mortality is significantly low in this cohort compared with expectations based on US mortality patterns. Likewise, mortality from cancer and diseases of the circulatory, respiratory, digestive and genitorurinary systems was significantly less than expected. Fewer deaths resulted from injuries. These findings are indicative of a strong healthy worker effect among members of this cohort.

Table I. Mortality among white males employed by Los Alamos National Laboratory from 1943-1977

	Actual	Expected	SMR	95% C.I.
All causes of death	2182	3146.3	69	66 - 72
Cancers	482	656.1	73	67 - 80
Circulatory diseases	978	1521.3	64	60 - 68
Respiratory diseases	137	177.0	77	65 - 92
Digestive diseases	114	160.0	71	59 - 86
Genitourinary diseases	25	40.6	62	40 - 91
All injuries	299	373.8	80	71 - 90

Results for several site-specific cancers (Table 2) were especially interesting. Cancers of the rectum (SMR = 44, 95% confidence interval [C. I.] = 19 - 87), larynx (SMR = 31, 95% C. I. = 6 - 91), lung (SMR = 53, 95% C. I. = 44 - 64), kidney (SMR = 53, 95% C. I. = 24 - 101) and brain/central nervous system (SMR = 59, 95% C. I. = 31 - 100) were observed less often than expected. Leukemias were observed more often than expected (37 versus 26.3) for an SMR of 141 (95% C. I. = 99 - 194). Further investigation will need to be conducted to determine whether an association exists between these cases of leukemia and exposure to external ionizing radiation or plutonium.

The mortality analyses presented in this summary are preliminary. Analyses of mortality among members of this cohort will continue and will include an examination of the relationship between cause-specific mortality and exposures to external ionizing radiation and plutonium. These analyses are expected to be completed in 1991 with a detailed report prepared during 1992.

Table II. Cancer Mortality among white males employed by Los Alamos National Laboratory from 1943-1977

	Actual	Expected	SMR	95% C.I.
All cancers	482	656.1	73	67 - 80
Oral cancers	13	20.6	63	33 - 108
Digestive cancers	151	173.7	87	74 -102
Esophageal cancers	16	15.6	103	59 - 167
Stomach cancers	28	30.7	91	61 - 132
Colon cancers	47	57.2	82	60 -109
Rectal cancers	8	18.2	44	19 - 87
Liver/gallbladder cancers	9	12.9	70	32 - 132
Pancreatic cancers	38	34.5	110	78 - 151
Laryngeal cancers	3	9.6	31	6 - 91
Lung cancers	118	220.8	53	44 - 64
Bone cancers	3	3.0	100	20 - 293
Skin cancers	15	14.0	108	60 - 178
Prostatic cancers	27	36.6	74	49 -107
Testicular cancers	5	4.5	110	35 -257
Bladder cancers	13	16.8	77	41 - 132
Kidney cancers	9	16.9	53	24 - 101
Eye cancers	2	0.6	365	41 -1320
Brain/CNS cancers	13	22.2	59	31 - 100
Lymphosarcomas	14	13.2	106	58 - 178
Hodgkin's disease	9	8.6	104	48 - 198
Leukemias	37	26.3	141	99 - 194
Other lymphatic cancers	12	18.0	67	34 - 117
Benign neoplasms	5	9.1	55	18 - 128

Mortality among Zia Company Workers Monitored for Exposure to Plutonium and External Ionizing Radiation

Authors: Warren A. Galke and Emily R. Johnson
Group: Occupational Medicine, HSE-2
Funding Organization: Department of Energy, Office of Health and Environmental Research, Human Health and Assessments Division

After extensive data checking, an analytic file for Zia Company workers was created. It contains all persons employed by the Zia Company between April 1, 1946 (beginning of company) and the end of 1978 who were monitored for exposure to either plutonium or external ionizing radiation before the end of 1984. Of the 5424 subjects in the file, 2741 were monitored for plutonium and 5200 were monitored for external ionizing radiation. Not everyone who was monitored for plutonium was monitored for external ionizing radiation. This population is referred to as the radiation-monitored subcohort to distinguish it from the full cohort, which is not yet ready for analysis.

The radiation-monitored subcohort was predominantly male and white. Of those for which we know sex and race, only 365 were female and 116 were nonwhite. There was no missing data for sex and less than 10% missing data for race. By the end of study in 1984, the population was aging, as evidenced by the mean birth year of 1926. Less than 10% of the population was born as late as 1950. The mean hire date for this group was 1958 with a large proportion of people (45%) being employed for the first time in the 1940s.

We were able to ascertain vital status and retrieve death certificates for a significant portion of this population. Vital status was known for 97% of the population and less than 5% of possible death certificates were outstanding.

Regarding radiation exposure, we find that most persons were first monitored for plutonium in either the 1950s or the 1970s. Relatively few Zia Company workers fell into the exposed category of 2 or more nCi of plutonium body burden. Only 163 persons on record have ever had a body burdens of 2 nCi for plutonium-239; the numbers of individuals exposed to 5 nCi and 10 nCi were 81 and 26, respectively. Exposures to plutonium-238 were even lower; seven had a body burden of 2 nCi and one had a body burden of 10 nCi.

By the end of study, 367 subjects had accumulated between 1 and 5 rem of external ionizing radiation. Sixty-four more subjects had accumulated between 5 and 10 rem and 63 had accumulated more than 10 rem.

We are currently analyzing the influence of radiation exposure on mortality in this population. The analyses completed thus far are for overall mortality within the population contained in the analytic file. The small number of minority and female subjects does not provide enough data for detailed examination of overall mortality by race and sex The table below summarizes overall mortality as measured by standardized mortality ratios (SMRs). Included in the table are the SMRs for all causes of death and all cancer deaths.

Race-Sex Group	Person Number	Person Years	SMR (95% C.I.) All causes	SMR (95% C.I.) All cancers
White males	4920	100633.2	79 (75 - 84)	79(69 - 90)
White females	354	7055.0	77 (50 -115)	78(33 - 153)
Black males	10	109.4	108 (1 -598)	0 (0 -2262)

As shown by this table, white males monitored for exposure to either plutonium or external ionizing radiation have a significantly lower mortality than the US population. White females show the same results although the confidence intervals are greater because of the smaller number in the analysis. Little can be said about the black males because the small sample precludes its use in statistical analysis.

Table I displays the cause-specific SMRs for the white males within the radiation-monitored subcohort. As is typically the case with industrial populations, the all-cause SMR is statistically low relative to the US general population (79, C. I. 75 - 84). Likewise, the all-cancer SMR is low (79, C. I. 69 - 90). Statistically significant elevated SMRs were found for stomach cancer, all injuries, all accidents, and motor vehicle accidents. The SMR for motor vehicle accidents was 199 with 95% C. I. of 155 - 251. The high SMRs for all injuries, all accidents, and motor vehicle accidents may reflect the statewide experience of New Mexico rather than a specific impact of employment with the Zia Company. According to an 1989 report, in 1985 the New Mexico death rate for all injuries was double that of the US. Furthermore, New Mexico ranks among the highest states for motor vehicle deaths. Stomach cancer mortality rates for New Mexico are also higher than US rates. Although not statistically elevated, the SMR of 312 found for bone cancer was interesting because this cancer in animals is known to be related to exposure to plutonium.

Table I. Mortality among white males employed by the Zia Company from 1946-1978 and monitored for exposure to either plutonium or external ionizing radiation

Cause	Observed	Expected	SMR	95% C.I.
All causes	1140	1440.83	79	75 - 84
All cancers	232	294.52	79	69 - 90
Oral cancers	4	9.04	44	12 - 113
Digestive cancers	78	81.73	95	75 - 119
Lung cancers	62	95.95	65	50 - 82
Blood cell cancers	30	27.69	108	73 - 155
Leukemias	15	11.37	132	74 - 218
Benign neoplasms	3	3.73	80	16 - 235
All genitourinary diseases	23	19.38	119	75 - 178
All injuries	155	116.42	133	113 - 156
All accidents	118	78.37	151	125 - 180
Motor vehicle accidents	70	35.25	199	155 - 251
Suicide	27	27.74	97	64 - 142

Environmental Surveillance

Depleted Uranium Investigations at Elgin Air Force Base, Florida

Author: Naomi M. Becker
Group: Environmental Protection, HSE-8
Funding Organization: US Air Force

Ongoing studies in collaboration with the US Air Force are designed to understand and characterize the nature of depleted uranium transport at Eglin Air Force Base, Florida. Since the late 1960s, Eglin Air Force Base has been the site of research, development, testing, and evaluation of munitions containing depleted uranium, beginning with the open-air testing of depleted uranium penetrators.

Research began with analysis of Eglin's soils to understand uranium partitioning by particle size. Size distribution is important when formulating models that simulate particle transport by water or air.

Uranium leaching investigations of Eglin soils were performed to define the rate at which uranium in the particulate phase will leach into the dissolved phase. Uranium was observed to leach rapidly and readily into the dissolved phase, especially at high initial uranium concentrations.

Both of these investigations contribute a great deal to the understanding of how uranium migrates in the hydrologic environment. The Eglin studies concentrate on uranium transport in a humid climate and provide a basis for comparison with similar studies conducted in the semiarid climate of Los Alamos.

Movement of Depleted Uranium by Sediment Transport Mechanisms

Author: Naomi M. Becker
Group: Environmental Protection, HSE-8
Funding Organizations: M Division and HSE Division

Sediment transport studies, begun in 1983, were initiated to investigate the rate of movement of depleted uranium that is aerially deposited by dynamic weapons component testing, which began in the 1940s. The area studied is a small semiarid watershed at LANL. Depleted uranium is isotopically distinguishable from naturally occurring uranium found in rock and sediment. This aspect of depleted uranium enables it to be used as a convenient tracer for elucidating sediment transport kinematics in a region typified by rapid aggradation and degradation.

Sampling strategies were developed to investigate flow and sediment transport processes. These methods were developed to be robust, inexpensive, operable without power, and reliable.

Several unique features within the watershed are apparent: 1) there is no perennial flow; when flow occurs, it is event-driven; and flow is discontinuous, both temporally and spatially; and 2) although the watershed is small (<800-ha area; 8-km long), flow and sediment discharge do not travel the entire length of the watershed for the majority of precipitation/flow events. These features have created interesting depositional patterns and unexpected implications for localized recharge and contaminant transport potential.

Los Alamos Climatology

Author: Brent M. Bowen
Group: Environmental Protection, HSE-8
Funding Organization: HSE Division

The Los Alamos Climatology Report, published annually, presents Los Alamos climate data and analyses of basic meteorological variables from late 1910 through 1989. The first section summarizes Los Alamos climate. Temperature, humidity, and precipitation analyses are given in the next few sections, with daily temperature and precipitation records listed and analyzed from late 1910. More detailed records of temperature and humidity, as well as winds, pressure, insolation, and other weather phenomena, are analyzed and discussed in later sections for the years 1980-1988, followed by a section on historical climate trends in Los Alamos. The last part of the report is directed to readers desiring more technical information. One section is devoted to weather extremes, another presents climate records and variability, and two others deal with topics important in air pollution meteorology: (1) dispersion and (2) wind persistence and turbulence. The appendices include sections on historical locations of weather stations, future plans of the Laboratory's Meteorology Section, and data quality and accuracy. Unit conversions, psychometric tables, and wind-chill equivalence charts also appear in the appendices. The report ends with a glossary of weather terms.

Environmental Monitoring with the National Park Service

Authors: Craig F. Eberhart and David Jardine
Group: Environmental Protection (HSE-8)
Funding Organization: HSE Division

Los Alamos National Laboratory continued to monitor ambient air quality at TA-49 during 1990 to evaluate the potential impact of Laboratory operations on Bandelier National Monument. Laboratory personnel use continuous ambient air monitoring instrumentation to measure sulfur dioxide, nitrogen dioxide, ozone, and visibility. Inhalable particulate matter samples are collected every six days. Weekly precipitation samples are collected as part of the National Atmospheric Deposition Program. The pH, conductivity, and volume of the precipitation samples are measured and results sent to the Central Analytical Laboratory in Illinois for cation and anion analyses.

Wetland Characterization and Utilization Studies at Pajarito and Sandia Canyons

Authors: Teralene S. Foxx, Kathryn Bennett, Joan Morrison, Brenda Edeskuty, and Timothy Haarmaan
Group: Environmental Protection, HSE-8
Funding Organization: Los Almos National Laboraoty, Environmental Restoration

Wetlands are semiaquatic and are inundated or saturated by water for varying periods of time during the growing season. These areas provide conditions necessary for the growth of specially adapted plants (hydrophytes) and, because of inundation, cause development of characteristic soils (hydric). These areas are valuable natural resources that provide numerous benefits for the environment including food and habitat for wildlife, flood protection, and erosion control in addition to aesthetic beauty for human enjoyment. Wetlands are critical to the survival of many animals including some amphibians, birds,reptiles, and mammals. The alarming rate of loss of wetlands throughout the United States has spurred concern over loss of biodiversity as well as loss of habitat for sensitive species.

These concerns have led the Los Alamos National Laboratory, in coordination with the United States Fish and Wildlife Service (USFW), to map all wetlands greater than one acre within Laboratory boundaries. The mapping, part of the USFW National Wetlands Inventory (NWI), uses a protocol of aerial maps and a hierarchical classification based on ecological, hydrological, and substrate characteristics.

To further understand the condition and complexity of the wetlands identified in the NWI, a wetlands characterization and utilization study was begun during 1990. Two wetlands classified as marshes in Sandia and Pajarito canyons were selected for the initial year of study. The wetlands within Sandia Canyon are maintained by effluent flow, and the wetlands within Pajarito Canyon are largely maintained by surface runoff and seeps.

Results of the first year of study indicate that these wetlands provide essential habitat for a number of species, including the chorus frog (*Pseudacris triseriata*), canyon treefrog (*Hyla arenicolor*), spadefoot toad, (*Scaphiopus multiplicaus*), woodhouse toad (*Bufo woodhousei*), manylined skink (*Eumeces multivirgatus*), and Great Plains skink (*Eumeces obsoletus*). In addition, these areas are used by elk (*Cervus canadensis*), raccoon (*Procyon lotor*), coyote (*Canis latrans*), bobcat (*Lynx rufus*), and a variety of small mammals. Raptor species, including the American kestrel (*Falco sparverius*) and redtail hawk (*Buteo jamaicensis*) use the areas for foraging, and a number of song birds use the wetlands for nesting as well as foraging. Quantitative data were collected on use patterns and densities of reptiles, amphibians, and small mammals as compared to the adjacent upland habitat. Other quantitative studies included monitoring water quality, aquatic invertebrates, vegetation analysis, and determination of hydric soils and soil quality.

Because of the importance of the wetland habitats to wildlife inhabiting Laboratory property, additional wetland studies will be conducted during 1991.

Publications

Industrial Hygiene (HSE-5)

S. D. Arnold and G. M. Talley, RHealth and Safety Guide for Inorganic Compounds and Metals Used in the Fabrication of Superconductive Alloys,S Los Alamos National Laboratory report LA-UR-90-1329 (April 1990).

O. D. Bradley, RRemotely Controlled Timed Air-Sampling System,S 1990 American Industrial Hygiene Conference, Orlando, Florida, May 13-18, 1990.

C. I. Fairchild, RWinds of Change for Plutonium Laboratories,S in RLos Alamos National Laboratory Research Highlights 1989,S Los Alamos National Laboratory report LALP-89-42 (March 1990), p. 42.

L. M. Holland, RCrystalline Silica and Lung Cancer: A Review of Recent Experimental Evidence,S *Regulatory Toxicology and Pharmacology* **12**, 224-237 (1990).

T. C. Hower and K. D. Blehm, RInfrared Thermometry in the Measurement of Heat Stress in Firefighters Wearing Protective Clothing,S *Appl. Occup. Environ. Hyg.* **5**, 782-786 (1990).

S. K. Rector and J. F. Stampfer, REffects of Reuse on the Performance of Chemical Protective Clothing,S in 1990 American Industrial Hygiene Conference, Orlando, Florida, May 13-18, 1990.

R. C. Scripsick and W. C. Hinds, RPerformance of Fibrous Filters at Low Flow Rates,S in *Aerosols: Science, Industry, Health, and Environment*, Senichi Masuda and Kanji Takahashi, Eds. (Pergamon Press, Tokyo, 1990) Vol. 2, pp. 821-824.

G. O. Wood, RCorrelations of Adsorption Isotherm Parameters for Activated Carbons,S in *International Carbon Conference* (GFEC, Paris, France, 1990) pp. 104-105.

G. O. Wood, RAdsorption Bed Breakthrough Curve Data Fitting,S in *R*Proceedings of the 1989 US Army Chemical Research, Development, and Engineering Center Scientific Conference on Chemical Defense Research,S US Army report CRDEC-SP-024 (August 1990).

Waste Management (HSE-7)

L. Christensen, RA Training Data Base,S Los Alamos National Laboratory report LA-UR-90-4074.

H. W. Kopp, RThe Impact of WIPP Delays on TRU Waste Management at Los Alamos National Laboratory,S Los Alamos National Laboratory report LA-UR-90-4075.

A. J. Montoya, E. Williams, Y. Tang, and I. Chen, R Computer-Based Data Systems for Managing Chemical Wastes at Los Alamos National Laboratory,S Los Alamos National Laboratory report LA-UR-90-4076.

G. M. Montoya, RDecommissioning a Nuclear Reactor,S Los Alamos National Laboratory report LA-UR-90-4077.

N. N. Sauer, K. D. Elsberry, W. Van Der Sluys, J. Watkin, D. Ehler, and G. Lussiez, RTreatment of Reactive Uranium-238 Chips and Turnings for Waste Minimization and Recycle,S Los Alamos National Laboratory report LA-UR-90-4173.

J. Weinrach, B. Myers, and P. Josey, RImplementing a Comprehensive Waste Minimization Policy at Los Alamos National Laboratory,S Los Alamos National Laboratory report LA-UR-90-4078.

Environmental Protection (HSE-8)

L. E. Bate, B. M. Gallaher, C. Barber, and G. J. Syme, RRisk Analysis of Underground Storage Tank Leakage Using Geographic Information System Technology,S *Proceedings of the 1990 Pacific Basin Conference on Hazardous Waste*, November 1990 (Honolulu, Hawaii).

B. M. Bowen, Los Alamos Climatology, Los Alamos National Laboratory report LA-11735-MS (May 1990).

M. J. Chapman, B. M. Gallaher, and D. A. Early. RA Preliminary Investigation of the Hydrogeology and Contamination in the Area of an Abandoned Manufactured Gas Plant in Albany, Georgia,S Water Resources Investigations report 90-141 (1990).

E. S. Gladney, and R. W. Ferenbaugh, RAn Investigation of the Impact of Inorganic Air Pollutants on Saguaro National Monument, Tucson, Arizona,S Seminar presented at Northern Arizona University (October, 1990).

E. S. Gladney, and I. Roelandts, R1988 Compilation of Elemental Concentration Data for CCRMP Reference Rock Samples SY-2, SY-3, and MRG-1,S *Geostandards Newsletter* **14**, 373-458 (1990).

E. S. Gladney, and I. Roelandts, R1988 Compilation of Elemental Concentration Data for USGS Geochemical Exploration Reference Materials GXR-1 to GXR-6,S *Geostandards Newsletter* **14**, 21-11 (1990).

J. L. Morrison, RThe Meadow Jumping Mouse in New Mexico: Habitat Preferences and Management Recommendations,S in *Managing Wildlife in the Southwest*, P. R. Krausman and N. S. Scott, Eds. (The Wildlife Society, Phoenix, Arizona, October 1989) p. 136.

W. D. Purtymun, R. J. Peters, and M. N. Maes, RPlutonium Deposition and Distribution from Worldwide Fallout in Northern New Mexico and Southern Colorado,S Los Alamos National Laboratory report LA-11794-MS (August 1990).

W. D. Purtymun, R. J. Peters, and M. N. Maes, RTransport of Plutonium in Snowmelt Runoff,S Los Alamos National Laboratory report LA-11795-MS (July 1990).

W. D. Purtymun, and A. K. Stoker, RPerched Zone Monitoring Well Installation,S Los Alamos National Laboratory report LA-UR-90-3230 (September 1990).

R. Raymond, E. S. Gladney, D. L. Bish, A. D. Cohen, and L. M. Maestas, RVariation of Inorganic Contents of Peats with Depositional and Ecological Settings,S in *Recent Advances in Coal Geochemistry*, L. L. Chyi and C. L. Chou. Eds., Geological Society of America special paper 248, pp. 1-12 (1990).

K. W. Sims, H.E. Newsom, and E. S. Gladney, RChemical Fractionation during Formation of the EarthUs Core and Continental Crust: Clues from As, Sb, W, and Mo,S in *Origin of the Earth*, Newsom, Ed.(Lunar and Planetary Institute, Houston, Texas, 1990), pp. 291-317.

L. F. Soholt, REnvironmental Surveillance of Low-Level Radioactive Waste Management Areas at Los Alamos during 1987,S Los Alamos National Laboratory report LA-UR-90-3283 (November 1990).

A. K. Stoker, RPerched Zone Monitoring Wells Analytical Results,S Los Alamos National Laboratory report LA-UR-90-4300 (December 1990).

G. Stone, and D. Hoard, RAn Anomalous Wind Between ValleysQIts Characteristics and a Proposed Explanation,S Fifth Conference on Mountain Meteorology, Boulder, Colorado, June 25-29, 1990, American Meteorological Society preprint, pp. 209-215.

G. Stone, and D. Hoard, RDaytime Wind in Valleys Adjacent to the Great Salt Lake,S Fifth Conference on Mountain Meteorology, Boulder, Colorado, June 25-29, 1990, American Meteorological Society preprint, pp. 216-223.

Health and Environmental Chemistry (HSE-9)

W. S. Baldridge, F. V. Perry, D. T. Vaniman, L. D. Nealey, B. K. Leavy, A. W. Laughlin, P. Kyle, Y. Bartov, G. Steinitz, and E. S. Gladney, RMiddle to Late Cenozoic Magmatism of the Southeastern Colorado Plateau and Central Rio Grande Rift (New Mexico and Arizona, USA): A Model for Continental Rifting,S (to be published in *Tectonophysics*).

M. H. Ebinger, E. H. Essington, E. S. Gladney, B. D. Newman, and C. L. Reynolds, RLong-Term Fate of Depleted Uranium at Aberdeen and Yuma Proving Grounds Final Report, Phase I: Geochemical Transport and Modeling,S Los Alamos National Laboratory report LA-11790-MS (June 1990).

R. W. Ferenbaugh, E. S. Gladney, and G. H. Brooks, Jr., RSigma Mesa: Background Elemental Concentrations in Soil and Vegetation, 1979,S Los Alamos National Laboratory report LA-11941-MS (October 1990).

M. A. Gautier, E. S. Gladney, E. A. Jones, M. Phillips, N. Koski, and B. T. OUMalley, Quality Insurance for Health and Environmental Chemistry: 1989,S Los Alamos National Laboratory report LA-11995-MS (Dec. 1990).

E. S. Gladney, E. A. Jones, E. J. Nickell, and I. Roelandts, R1988 Compilation of Elemental Concentration Data for USGS BCR-1,S *Geostandards Newsletter* **14**, 209-359 (1990).

E. S. Gladney and I. Roelandts, R1988 Compilation of Elemental Concentration Data for CCRMP Reference Rock Samples SY-2, SY-3, and MRG-1,S *Geostandards Newsletter* **14**, 373-458 (1990).

E. S. Gladney and I. Roelandts, R1988 Compilation of Elemental Concentration Data for USGS Geochemical Exploration Reference Materials GXR-1 to GXR-6,S *Geostandards Newsletter* **14**, 21-118 (1990).

K. G. W. Inn, W. S. Liggett, Jr., H. L. Volchok, M. S. Feiner, J. F. McInroy, D. S. Popplewell, D. R. Percival, R. A. Wessman, V. T. Bowen, H. D. Livingston, R. L. Kathren, and H. Kawamura, RInterlaboratory Comparison of Actinides in Human Tissue, ^{239}Pu and ^{240}Pu,S *Journal of Radioanalytical and Nuclear Chemistry* **138** (2), 219-229, (1990).

R. L. Kathren, and J. F. McInroy, RComparison of Systemic Plutonium Deposition Estimates from Urinalysis and Autopsy Data in Five Whole Body Donors,S *Health Phys* **60** (4) (1991), pp. 481-488.

R. L. Kathren and J. F. McInroy, RImplications of Postmortem Human Tissue Analysis on Biokinetic Models for Actinides,S Third International Conference on the Measurement of Actinides and Long-Lived Radionuclides in Biological and Environmental Samples, Bombay, India, January 29-February 2, 1990. (submitted to *International Journal of Radioanalytical and Nuclear Chemistry*).

R. L. Kathren, D. J. Strom, J. F. McInroy, and R. E. Bistline, RDistribution of Plutonium and Americium in the Lungs and Lymph Nodes of United States Transuranium Registrants and Relationship to Smoking Status,S *Health Phys* **58**, S48 (1990).

J. F. McInroy, RDistribution of Plutonium in Man,S *Health Phys* **58**, S6 (1990).

J. F. McInroy and R. L. Kathren, RPlutonium Content in Marrow and Mineralized Bone in an Occupationally Exposed Person,S *Radiation Protection Dosimetry* **32** (4) 245-252 (1990).

J. F. McInroy, R. L. Kathren, G. L. Voelz, and M. J. Swint, R US Transuranium Registry Report on the ^{239}Pu Distribution in a Human Body,S Health Phys **60** (3) 307-333 (1991).

J. M. McInroy, J. J. Miglio, E. R. Gonzales, M. J. Swint, and R. L. Kathren, RDistribution of ^{238}Pu in a Whole Body Donated to the US Transuranium Registry,S Third International Conference on the Measurement of Actinides and Long-Lived Radionuclides in Biological and Environmental Samples, Bombay, India, January 29-February 2, 1990 (submitted to *International Journal of Radioanalytical and Nuclear Chemistry*).

R. Raymond, E. S. Gladney, D. L. Bish, A. D. Cohen, and L. H. Maestas, RVariation of Inorganic Contents of Peats with Depositional and Ecological Settings,S in *Recent Advances in Coal Geochemistry*, L. L. Chyi and C. L. Chou, Eds., Geological Society of America, Special Paper 248, pp.J1-12 (1990).

K. Shiraishi, J. F. McInroy, and Y. Igarashi, RSimultaneous Multielement Analysis of Diet Samples by Inductively Coupled Plasma Mass Spectrometry and Inductively Coupled Plasma Atomic Emission Spectrometry,S *J. Nutr. Sci. Vitaminol.* **36**, 81-86 (1990).

K. W. Sims, H. E. Newsom, and E. S. Gladney, RChemical Fractionation During Formation of the EarthUs Core and Continental Crust: Clues from As, Sb, W, and Mo,S in *Origin of the Earth*, Newsom, Ed. (Lunar and Planetary Institute, Houston, Texas, 1990), pp.J291-317.